Virology 391 (2009) 5–19

Contents lists available at ScienceDirect

Virology

journal homepage: www.elsevier.com/locate/yviro

Immune evasion proteins gpUS2 and gpUS11 of human cytomegalovirus incompletely protect infected cells from CD8 T cell recognition

K. Besold [a], M. Wills [b], B. Plachter [a,*]

[a] Institute for Virology, University Medical Center, Johannes Gutenberg-University Mainz, Obere Zahlbacher Str. 67, D-55131 Mainz, Germany
[b] Department of Medicine, University of Cambridge Clinical School, Hills Rd, Cambridge, CB2 2QQ, UK

ARTICLE INFO

Article history:
Received 22 October 2008
Returned to author for revision 6 May 2009
Accepted 1 June 2009
Available online 30 June 2009

Keywords:
Cytomegalovirus
Immune evasion
US2
US11
MHC class I
pp65
IE1
CTL

ABSTRACT

Human cytomegalovirus (HCMV) encodes four glycoproteins, termed gpUS2, gpUS3, gpUS6 and gpUS11 that interfere with MHC class I biosynthesis and antigen presentation. Despite gpUS2–11 expression, however, HCMV infection is efficiently controlled by cytolytic CD8 T lymphocytes (CTL). To address the role of gpUS2 and gpUS11 in antigen presentation during viral infection, HCMV mutants were generated that expressed either gpUS2 or gpUS11 alone without coexpression of the three other proteins. Fibroblasts infected with these viruses showed reduced HLA-A2 and HLA-B7 surface expression. Surprisingly, however, CTL directed against the tegument protein pp65 and the regulatory IE1 protein still recognized and lysed mutant virus infected fibroblasts. Yet, suppression of IE1 derived peptide presentation by gpUS2 or gpUS11 was far more pronounced. The results show that gpUS2 and gpUS11 alone only incompletely protect HCMV infected fibroblasts from CTL recognition and underline the importance of studying infected cells to elucidate HCMV immune evasion.

Introduction

Infection with the human cytomegalovirus (HCMV) may lead to severe and life threatening disease conditions in individuals with impaired or immature immune defense functions. In contrast, HCMV infection is readily controlled by the immune system in healthy individuals, rarely leading to overt clinical manifestations (Mocarski et al., 2007). Both in murine models and in clinical studies, it could be shown that cytolytic CD8 T lymphocytes (CTL) are major immunologic effectors that mediate protection against CMV disease (Reddehase et al., 1987; Walter et al., 1995). However, despite the obvious efficiency of CMV specific CTL, these cells cannot prevent the establishment of viral latency. Latent infection may be interrupted by episodes of reactivation, which again are controlled by CTL (Simon et al., 2006). CMV infections are thus characterized by an intricate balance between an efficient immune surveillance by the host and CMV specific mechanisms that help the virus to evade complete immune control and eradication.

HCMV has evolved multiple strategies to interfere with both the innate and the adaptive immune response of its host. These topics have been covered by recent reviews (Braud et al., 2002; Lilley and Ploegh, 2005; Mocarski, 2004; Reddehase, 2002; Tortorella et al., 2000). Major interest of research has focused on the impairment of recognition of infected cells by CTL. Early work described down-modulation of major histocompatibility complex class I (MHC class I) molecules on the surface of HCMV infected human fibroblasts (HF) (Barnes and Grundy, 1992), leading to an impairment of CTL mediated cytolysis (Khan et al., 2005; Manley et al., 2004). Deletion mutagenesis identified a region on the 230 kbp DNA genome of HCMV, encompassing the putative open reading frames US2 to US11, which genetically defined the MHC class I downmodulation phenotype of the virus (Jones et al., 1995). In this latter work, Jones et al. specified the US11 gene as one, but not the sole determinant that affected MHC class I biogenesis in HCMV infected cells. Later investigations additionally defined the proteins encoded by US2, US3 and US6 to independently mediate MHC class I downregulation in cells expressing the individual genes (Ahn et al., 1996; Ahn et al., 1997; Jones et al., 1996; Wiertz et al., 1996b). The four gene products gpUS2, gpUS3, gpUS6 and gpUS11 (herein concisely termed gpUS2–11) were thus defined as immune evasins.

The gpUS2 and gpUS3 have also been found to interfere with MHC class II antigen presentation (Hegde et al., 2002; Tomazin et al., 1999), and gpUS2 was reported to cause degradation of the nonclassical class I MHC complex molecule HFE (Ben-Arieh et al., 2001). Furthermore, variations in the efficiency of MHC class I downmodulation by gpUS2–11 after infection of different cell types have been described (Rehm et al., 2002; Schust et al., 1998). In particular, the efficiency of gpUS2–11 in downmodulating MHC class I and class II in professional antigen presenting cells may be limited, which may explain the efficient priming of an antiviral immune response despite immune evasion. Recent evidence from murine CMV (MCMV) infection even point to an enhancing effect of the homologous MCMV proteins on priming

* Corresponding author. Fax: +49 6131 393 3652.
E-mail address: plachter@uni-mainz.de (B. Plachter).

0042-6822/$ – see front matter © 2009 Elsevier Inc. All rights reserved.
doi:10.1016/j.virol.2009.06.004

(Böhm et al., 2008). In the effector phase of the immune response, i.e. during the acute or reactivated infection, HF support HCMV replication (Sinzger et al., 1995). These cells are thus a major target of antiviral CD8 T cells in order to limit infection. Consequently, investigating the effect of gpUS2–11 after infection of HF provides important information about the role of evasion for the control of infection.

MHC class I molecules are heterotrimeric complexes consisting of a variant heavy chain, the invariant β2-microglobulin chain and an antigenic peptide (Townsend et al., 1989). These peptides are derived from cellular or viral proteins, which are degraded in the cytosol by proteasomes and are transported by the transporter associated with antigen presentation (TAP) into the lumen of the ER (Yewdell and Bennink, 2001). Peptides with appropriate lengths and binding motifs are then loaded onto particular MHC class I molecules, a process mediated by ER-resident chaperons (Bouvier, 2003). Assembled MHC class I complexes are subsequently transported to the cell surface, where they engage with antigen specific T cell receptors on CTL, leading to the activation of the effector functions of these lymphocytes (Heemels and Ploegh, 1995).

The viral glycoproteins gpUS2, gpUS3, gpUS6 and gpUS11 have been shown to interfere at various stages with this process of MHC class I biosynthesis (reviewed in Lilley and Ploegh, 2005; Loenen et al., 2001; Powers et al., 2008; Reddehase, 2002). The early proteins gpUS2 and gpUS11 both mediate the dislocation of MHC class I heavy chains (HC) to the cytosol, where the latter proteins are degraded by the proteasome (Wiertz et al., 1996b, 1996a). However, gpUS2 and gpUS11 differ in several ways with respect to their interaction with HC and the mechanisms, by which they induce cytoplasmic translocation of MHC class I molecules (reviewed in Lilley and Ploegh, 2005; Powers et al., 2008). The gpUS2 contacts the HC between the peptide binding groove and the α3-domain (Gewurz et al., 2001a). The interaction domain is intrinsic for only a portion of the human HLA allomorphs, implying allele specific degradation mediated by gpUS2 (Barel et al., 2003b; Gewurz et al., 2001b). In contrast, gpUS11 appears to bind to the α1–2-domains of HC, which renders the viral protein less specific in its capabilities to induce degradation of different HLA allomorphs (Barel et al., 2003a). Furthermore, gpUS2- and gpUS11-mediated translocation of HC requires different cellular factors (Lilley and Ploegh, 2004; Loureiro et al., 2006). Finally, gpUS2 only acts on HC that have been correctly folded, whereas gpUS11 degrades free HC or HC-β2m complexes (Gewurz et al., 2001a; Lilley and Ploegh, 2005). All of this together indicate that gpUS2 and gpUS11 have evolved to target different cellular pathways in order to achieve the same goal, namely translocation and degradation of MHC class I molecules during HCMV infection.

The gpUS2 and gpUS11 have been instrumental for our understanding of the mechanisms of ER protein quality control and protein dislocation from the ER to the cytosol. On the other hand, a lot has been learned about the molecular interaction of the two proteins with the MHC class I pathway (reviewed in detail in Lilley and Ploegh, 2005). Sole expression of gpUS2 or gpUS11 interferes with MHC class I biosynthesis in HCMV infected fibroblasts (Jones et al., 1995; Jones and Sun, 1997). In addition, infection with HCMV mutants that expressed either gpUS2 or gpUS11 mediated degradation of HC that had been accumulated in the ER of gpUS3 expressing U373-MG cells (Jones and Sun, 1997). A cooperative effect of gpUS2 and gpUS3 was recently shown by coexpression of the two proteins in U373-MG cells (Noriega and Tortorella, 2009). Infection with gpUS2/US3pos or gpUS6/US11pos HCMV mutants resulted in MHC class I downregulation at 24 h p.i. and moderate to intermediate reduction of infected-cell cytolysis by HCMV specific CTL, compared to a US2–11 deletion mutant (Khan et al., 2005). However, one major unresolved issue is the role that gpUS2 and gpUS11 individually play to protect cells against recognition and cytolysis by CTL in the course of viral infection.

To address this question, mutants of HCMV were generated in which the open reading frames US3, US6 and US11 or US2, US3 and US6 were deleted sequentially from the viral genome. The resulting viral mutants expressed either gUS2 or gpUS11, but none of the three other immune evasins, respectively. All mutants retained the sequences encoding the open reading frames (orfs) US4–5 and US7–10 to be able to exclude any influences of these genes on MHC I presentation. Permissive human foreskin fibroblasts (HFF) infected with these mutants showed downregulation of HLA-A2 and HLA-B7. Yet, CTL directed against the immunodominant viral proteins pp65 and IE1 were still stimulated by HF infected with the mutant viruses, although to variable extent. Our results show that the impact of gpUS2 and gpUS11 expression in the absence of other MHC class I modulators of HCMV is remarkably limited, indicating that suppression of MHC class I antigen presentation by HCMV requires the concerted activity of all immune evasins.

Results

Generation of HCMV immune evasion mutants

The objectives of this work were to investigate the roles of gpUS2 and gpUS11, individually, in MHC class I downmodulation and protection against CTL recognition of HCMV infected cells. To be able to address this issue, viral mutants were generated in which the three other members of the US2–11 evasion genes of HCMV were removed from the viral genome. Furthermore, care was taken to retain the coding sequences for the US4–5 and US7–10 gene regions in the resulting viral recombinants. This appeared to be important as preliminary information from other laboratories on possible interactions of proteins encoded in the US7–10 region with MHC class I was available (Furman et al., 2002; Tirabassi and Ploegh, 2002). Mutagenesis of the viral genome in *Escherichia coli* was employed using the bacterial artificial chromosome (BAC) clone pAD/Cre (Brune et al., 2006; Lee et al., 2001; Yu et al., 2002). The Ad169 derived pAD/Cre contained the BAC vector and an expression cassette for the Cre recombinase, flanked by LoxP sites and inserted between the viral genes US28 and US29. Transfection of pAD/Cre derived clones into HFF leads to the site-specific excision of the BAC vector and the Cre gene in the course of viral reconstitution (Yu et al., 2002).

The orfs US3, US6 and US11 were deleted in sequential steps from pAD/Cre, using λ-Red recombination mediated genetic engineering (Recombineering; Lee et al., 2001; Mersseman et al., 2008b). The final BAC pKB13 consequently lacked the complete orfs (from start to stop codons) of US3, US6 and US11 (Fig. 1) and had a US2pos/US3neg/US6neg/US11neg genotype. An analogous BAC (pKB9) which only had the US11 orf retained was constructed using the same strategy (Fig. 1). This BAC was thus US2neg/US3neg/US6neg/US11pos. An additional mutant with precise deletion of all four orfs was generated for control (pKB6). All three BACs, pKB13, pKB9 and pKB6 retained the US4–5 and US7–10 gene regions.

The genomic structure of the recombinant BACs was analyzed by restriction endonuclease digestion (*Bam*HI) and agarose gel electrophoresis. The desired modifications in the genomic region of interest could be verified by shifts in the restriction pattern of the respective BAC clones (Fig. 1B). In addition, Southern blot analysis with US2, US3, US6 and US11 specific probes was used to verify the proposed genotype (Fig. 1C). DNA of pAD/Cre showed hybridization with probes specific for each of the four US genes. Hybridization with the US2 specific probe was only detectable in pKB13 DNA and US11 specific hybridization was only found in pKB9 DNA. No hybridization with the US2 and US11 probes was found in pKB6 DNA and hybridization with either a US3 or a US6 specific probe was undetectable in the DNA from any of the three mutants. In addition, the deletion of the respective genes was verified by PCR analysis and nucleotide sequencing of the BAC clones (data not shown). These analyses unequivocally proved that HCMV BACs that retained either US2 only, US11 only or none of the US2–11 evasion genes had been generated. The BAC DNAs were

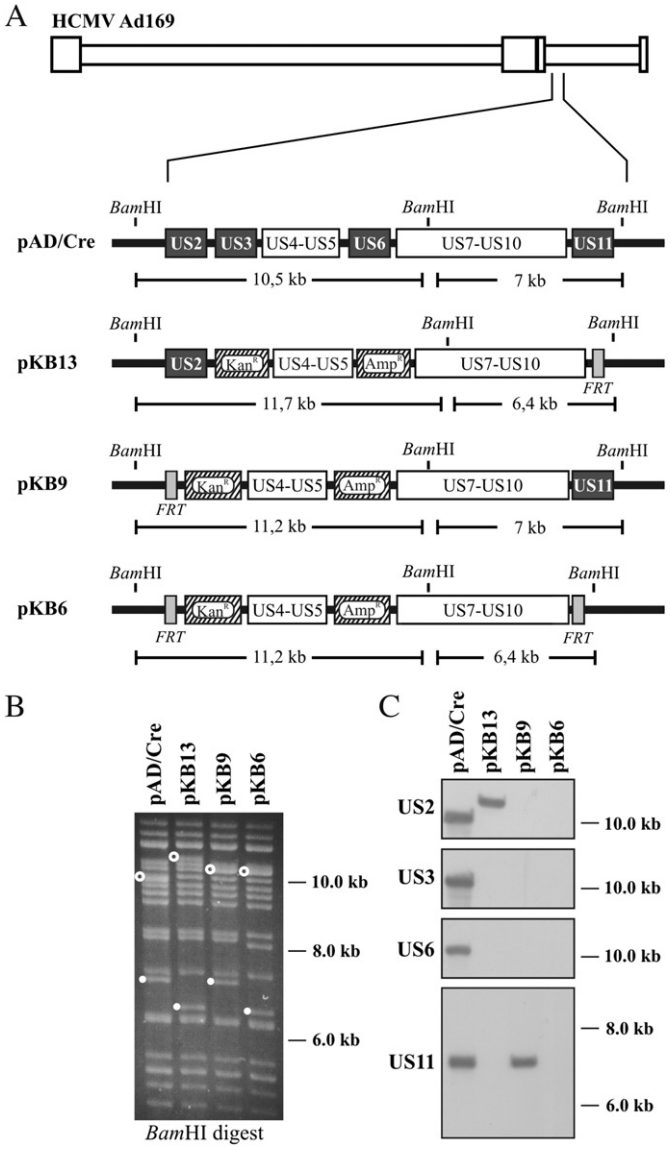

Fig. 1. Construction and verification of recombinant BACs. (A) Schematic representation of recombinant HCMV BACs. The genome of the Ad169 strain of HCMV with the location of the US2–11 gene region is shown on top. This region of interest is blown up in the maps below (not drawn to scale). The location of the orfs encoding US2, 3, 6 and 11 are shown by dark grey boxes. Restriction sites for *Bam*HI are indicated on top of each construct, the sizes of the fragments after digestion with *Bam*HI are shown below. Further to that, the Kan^R and Amp^R genes and the FRT sites used for constructing the BACs are also depicted. (B) Agarose gel electrophoresis of DNA of the different BACs, cleaved with *Bam*HI. The expected alterations in electrophoretic mobility of the 10.5 kb fragment of pAD/Cre are indicated by white circles, alterations of the 7 kb fragment are indicated by white dots. (C) Southern blot analysis of DNA from the different BACs, digested with *Bam*HI. The probes used for hybridization are indicated on the left side of each blot.

subsequently transfected into HFF and recombinant viruses were reconstituted (Borst et al., 1999).

Verification of the kinetics of replication and US2 and US11 gene expression of the viral mutants

One major focus of this study was to investigate the impact of gpUS2 and gpUS11 on antigen presentation at different time points after HCMV infection. The members of the US2–11 genes had been shown to be non-essential for replication in HFF (Dunn et al., 2003). However, a mutant lacking the genes US1–US15 had been reported to display a temperature-sensitive phenotype, indicating that important functions for viral replication were encoded in this region (Kollert-Jöns et al., 1991). It thus was mandatory to show that the mutant viruses generated here did not differ in their capacity to replicate in permissive cells and that the kinetics of expression of gpUS2 and gpUS11, respectively was comparable to the wild type (wt) situation.

In a first step, single cycle growth kinetics were analyzed to test the capacity of the different viral strains to release infectious viral progeny. HFF were infected with the various mutants at an moi of 5. Cell culture supernatants were analyzed for infectivity at different time points p.i. by quantifying IE1 positive cells 48 h after infection with the different supernatants (Fig. 2A). The release of IE1 forming units was comparable between wt virus RV-BADwt and the 3 different viral strains, showing that there was no impairment of any of the mutant strains to pass through the viral replication cycle.

To study viral replication in more detail, in a second step initiation and course of viral DNA replication was analyzed using TaqMan PCR on DNA, isolated from HFF at different time points after infection with the various mutants (Fig. 2B). Levels of viral DNA of the mutants at different times p.i. were comparable to the DNA-levels of the wt virus RV-BADwt showing that the mutants were not impaired in their fitness to replicate in permissive cells. Finally, the release of DNA-containing particles from HFF was measured using TaqMan PCR quantification of viral DNA, isolated from infected cell culture supernatant at different times after infection (Fig. 2C). The amount of DNA detectable at each time point tested was indistinguishable between each of the individual mutants and RV-BADwt. This indicated that the mutants were unimpaired in their synthesis and release of viral progeny.

To verify that the expression kinetics of US2 and US11 in cells infected with the mutants was comparable to that in wt HCMV infected cells, Northern blot analyses were performed. RNAs of 0.9 kb and 1.1 kb, respectively could be detected in total cell RNA preparations of RV-BADwt infected cells, using US2 or US11 specific probes (Fig. 3). The signals could first be detected at 6 h p.i. for both US2 and US11. Signal intensity reached a maximum at about 12 h p.i. and declined thereafter. Only vague signals were detectable at 72 h p.i.. Sizes of the fragments and kinetics of expression complied with previously published results, classifying US2 and US11 as being early–late genes (Chau et al., 1999; Jones and Muzithras, 1991; Jones and Sun, 1997).

Probing RNA from RV-KB13 infected cells with the US2 specific probe showed hybridization with the 0.9 kb RNA, as expected. Kinetics of expression of the US2 specific transcript was indistinguishable in RNA preparations from cells infected with RV-KB13 or the parental strain RV-BADwt (Fig. 3, upper panel). Using the US11 specific probe on RNA obtained from RV-KB9 infected cells showed the expected signal of 1.1 kb, with the same expression kinetics as detected in RV-BADwt infected cells (Fig. 3, lower panel). These blots confirmed that the genetic manipulations applied to delete the three other evasin genes did not alter the expression from the remaining genes US2 or US11. Finally, both the US2 and the US11 specific probes were hybridized to RNA obtained from RV-KB6 infected cells. As expected, no US2 or US11 RNA expression could be detected in RV-KB6 infected cells. Taken together, these results showed that the recombinant viruses displayed no apparent growth deficiency and that expression kinetics of the remaining evasin genes were conserved in the mutants.

gpUS2 and gpUS11 independently reduce MHC class I expression on infected cells

Early studies had shown that HF display a significant reduction of MHC class I surface expression during HCMV infection, as measured by flow cytometry (Barnes and Grundy, 1992). Deletion of US2–11 in recombinant viruses resulted in abrogation of this effect (Jones et al., 1995) and expression of only US2/US3 or US6/US11 by viral mutants showed intermediate downregulation of MHC I compared to that seen

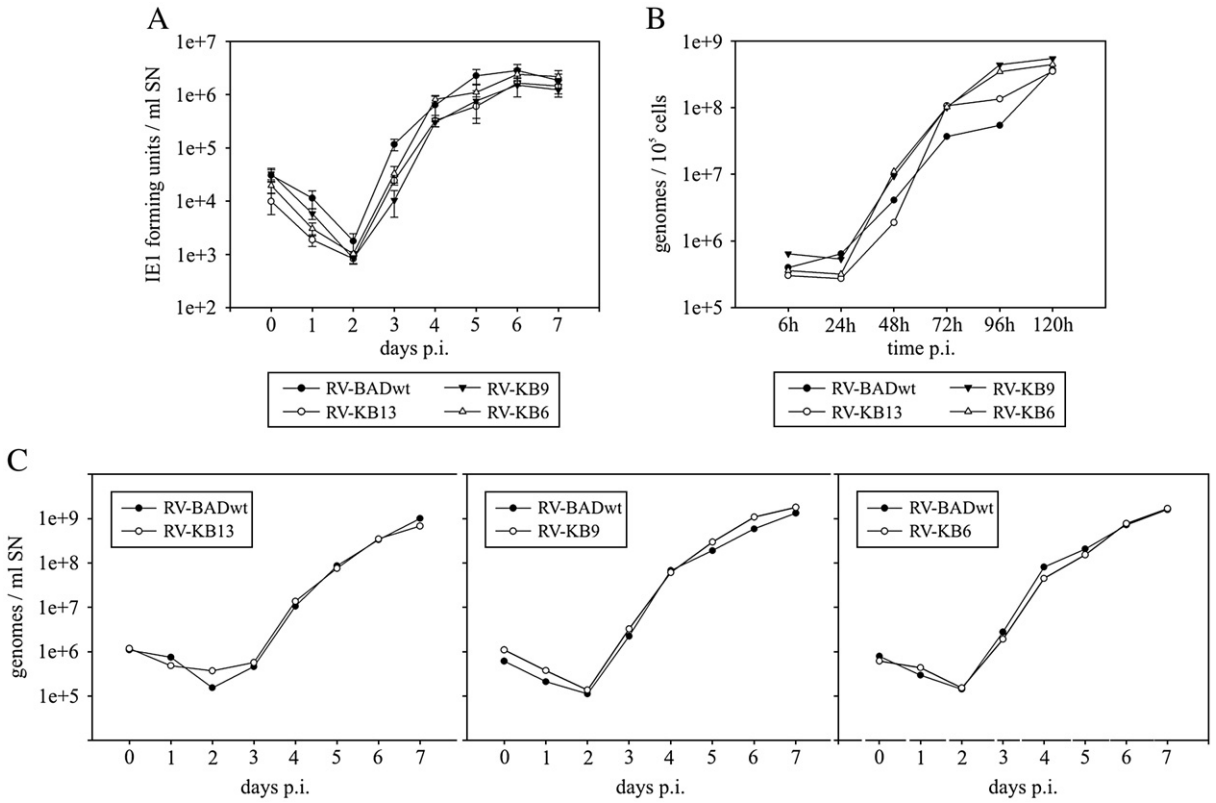

Fig. 2. Growth kinetics of the recombinant viral strains in comparison to the wild type strain RV-BADwt. HFF were infected with an moi of 5 (A) or with infectious culture supernatants that were normalized for an equivalent uptake of 4 viral genomes per cell (B, C). (A) Single cycle growth analysis of different viral mutants. At the indicated time points p.i., cell culture supernatants were harvested for quantification of viral titers by staining of infected fibroblasts for expression of the HCMV IE1 protein. Means and standard deviations for each data point were derived from 8 samples. (B) Kinetics of genome replication of the different viral mutants. At the indicated time points p.i., DNA was isolated from infected cells and the amount of viral DNA was measured using quantitative TaqMan DNA PCR analysis. (C) Kinetics of infectious, DNA-containing particle release from infected cells. At the indicated time points p.i., cell culture supernatants were collected. Viral DNA in each specimen was analyzed by quantitative TaqMan DNA PCR analysis. (B, C) Means of triplicate samples of one out of two independent experiments are shown in each case. SN, supernatant.

during wt infection (Khan et al., 2005). The impact of either gpUS2 or gpUS11 alone, however, on MHC class I surface expression of infected cells at different times p.i. remained unclear from these analyses. The availability of mutants expressing only gpUS2 or gpUS11 allowed us to ask the question about the contribution of each of the two evasins. HFF were infected for 1, 2, 3 and 4 days with the different viruses. Cells were subsequently analyzed by Fluorescence Activated Cell Sorting (FACS; Fig. 4A). As expected, cells infected with the gpUS2–11pos wt virus RV-BADwt showed a marked reduction of MHC class I surface expression, as measured using the HLA-ABC specific antibody W6/32. This was especially prominent at 2, 3 and 4 days p.i.. Infection with RV-KB13, expressing only gpUS2 of the four evasins gpUS2–11 (herein concisely termed US2pos virus) or RV-KB9, expressing only US11 (herein concisely termed US11pos virus), however, led to an only moderate reduction of HLA-ABC at different times p.i., as compared with uninfected cells. Surprisingly, this downregulation could not be enhanced by coinfection with RV-KB13 and RV-KB9.

For FACS analyses of MHC class I expression on the surface of infected cells, expression on uninfected cells is frequently used as a reference. It has been shown, however, that cells that are infected with a US2–11neg virus may even upregulate their MHC class I surface expression (Falk et al., 2002). We have also seen this in our experiments, using the US2–11neg virus RV-KB6 (Fig. 4A). It was thus conceivable that slight reductions of MHC class I mediated by gpUS2 or gpUS11 expression in infected cells were masked by this upregulation. Consequently we decided to use, for further experiments, RV-KB6 infected cells instead of uninfected cells as a reference (100%) for the expression of MHC class I on RV-BADwt, RV-KB13 or RV-KB9 infected cells. The results of three independent experiments are shown in Fig. 4B. Indeed a clear reduction of HLA-ABC on both RV-KB13 (US2pos) and RV-KB9 (US11pos) infected HFF became apparent, using this approach. This reduction was more pronounced in the later stages of infection. Neither gpUS2 nor gpUS11 expression alone, however, was sufficient to reduce MHC class I to levels, seen in wt virus (RV-BADwt) infected cells. These experiments showed that MHC class I surface expression on infected cells is impaired by gpUS2 or gpUS11 alone, but that this downregulation does not reach wt levels.

Both HLA-A2 and HLA-B7 are downregulated on gpUS2pos and gpUS11pos infected cells

gpUS2 and gpUS11 interact with different portions of MHC class I molecules in the ER (Barel et al., 2003a, 2003b; Gewurz et al., 2001a). The gpUS11 binding domain appears to be conserved between different HLA molecules. This was used to explain that gpUS11 could attack different HLA-A and HLA-B locus products (Barel et al., 2003a, 2003b; Lilley and Ploegh, 2005). In contrast, the residues of the binding site for gpUS2 on HLA-A2 are less well conserved in other HC (Barel et al., 2006; Gewurz et al., 2001a). This served as background for the finding that gpUS2 is not sufficient to attack certain HLA-B and HLA-C products, in particular HLA-B7 (Barel et al., 2003b, 2006; Llano et al., 2003). The latter investigations, however, were all carried out after transfection or retroviral transduction. To test the impact of gpUS2 and gpUS11 on HLA-A2 and HLA-B7 surface expression on infected cells, HFF were infected with either RV-KB13, RV-KB9 or coinfected with both viruses (Fig. 5). Surface expression of HLA-A2 or HLA-B7 was measured by FACS at different time points after infection. Again, HLA-A2 or HLA-B7 expression on cells infected with the US2–

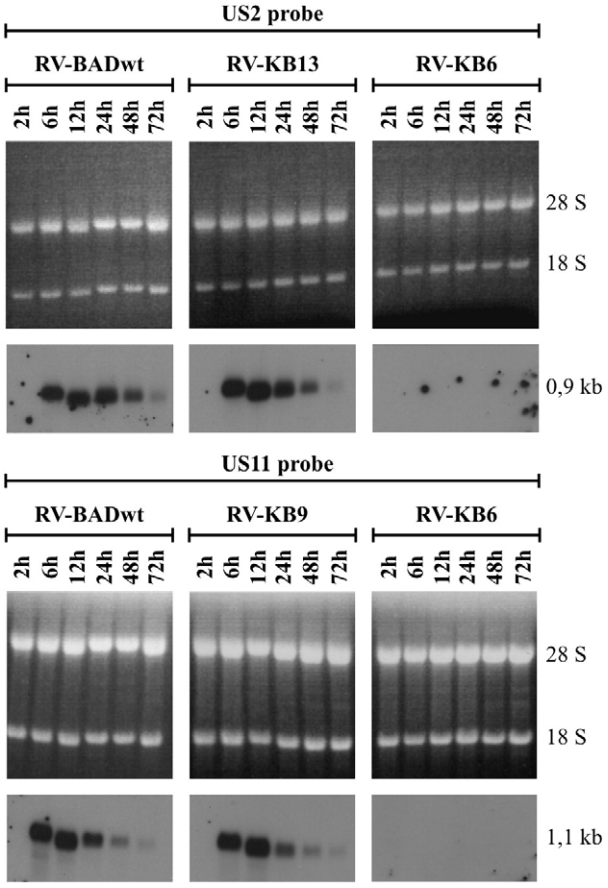

Fig. 3. Analysis of US2 and US11 RNA expression kinetics of parental and recombinant viral HCMV strains in the course of infection. HFF were infected with viral inocula that were normalized for an equivalent uptake of 125 viral genomes per cell. At the indicated time points p.i., total cellular RNA was isolated and subsequently separated by denaturing agarose gel electrophoresis (8 μg RNA per lane). After blotting, RNAs were hybridized to US2 (upper panel) and US11 specific (lower panel) probes. Positions of cellular 18S and 28S rRNAs are indicated on the right side of agarose gels. The rRNAs were taken as loading controls. Sizes of US2 and US11 transcripts are indicated on the right side of each blot. Cells infected with RV-KB6 were used as negative control.

11neg strain RV-KB6 was taken as 100%. As expected, both RV-KB13 (US2pos) and RV-KB9 (US11pos) downregulated HLA-A2 on HFF in the course of infection. Almost no signal above the background was detectable anymore at late stages of infection. An identical course of HLA-A2 expression was found when the cells were coinfected with RV-KB13 and RV-KB9 (Fig. 5A). These results confirmed that HLA-A2 was sensitive to either gpUS2 or gpUS11 attack. They further showed that both evasins were highly effective in downregulating HLA-A2 in HCMV infected cells.

The same experiments were carried out using an HLA-B7 specific antibody (Fig. 5B). Infection of HFF with RV-KB9 resulted in intermediate reduction of HLA-B7 in comparison to RV-BADwt infection. Downregulation of HLA-B7 was also seen after retroviral transduction of gpUS11 (Barel et al., 2006). In contrast to gpUS11, gpUS2 failed to downregulate HLA-B7 after ectopic expression of the evasin in transfected or transduced cells (Barel et al., 2003a, 2006; Gewurz et al., 2001b; Llano et al., 2003). To evaluate, whether HLA-B7 was also resistant against gpUS2 in infected cells, HFF were infected with RV-KB13 and tested by FACS analysis. Surprisingly, RV-KB13 infected HFF showed a pronounced reduction of HLA-B7 that was exceeding the reduction seen with RV-KB9 (Fig. 5B). The same level of reduction was seen after coinfection with both viruses. Identical results were obtained after RV-KB13 infection of two other HLA-B7 expressing HFF-lines (data not shown). Taken together these results demonstrated that the sole expression of gpUS11 in HCMV infected HFF has a strong downregulatory effect on HLA-A2 and a modest effect on HLA-B7 surface expression. Infection with the gpUS2pos mutant also leads to a marked downregulation of HLA-A2. Inconsistent with gpUS2-HLA-B7 coexpression experiments, however, infection of HLA-B7 positive HFF with the gpUS2pos mutant of HCMV led to a distinct reduction of B7 surface expression over time. The latter results underline the importance of studying the function of immunomodulatory HCMV proteins in the context of infection in order to define their role in evasion.

Infected HFF stimulate IFNγ secretion by pp65- and IE1-specific CTL despite gpUS2 or gpUS11 expression

Analysis of MHC class I surface expression levels by flow cytometry provides only limited information about the functionally relevant impact of immune evasion on CTL recognition. Small numbers of MHC class I peptide complexes on the cell surface, undetectable by the sensitivity of the FACS analysis, may be sufficient for CTL activation and, ultimately, for killing of the target cell. We thus investigated the role of gpUS2 and gpUS11 in functional antigen presentation by HCMV infected cells using IFN-γ Elispot analyses. CTL clones derived from HLA-A2 transgenic mice were used which were directed against immunodominant HLA-A2 presented peptides from the tegument protein pp65 and the regulatory IE1 protein of HCMV (Besold et al., 2007). In contrast to human CTL lines, these clones can be cultured indefinitely, thus enabling the repetition of experiments under comparable conditions.

We first tested the capacity of mutant virus infected HFF to present a pp65 derived peptide. Infected cells were subjected to Elispot analysis after various intervals p.i., using $pp65_{NLV}$-CTL [specific for the pp65 derived nonapeptide NLVPMVATV (Diamond et al., 1997); Fig. 6A]. At 24 h p.i., cells infected with the gpUS2pos virus RV-KB13 or the gpUS11pos virus RV-KB9 showed a slightly reduced percentage of spot numbers, as normalized to the numbers obtained with the gpUS2–11neg mutant RV-KB6 (taken as 100%). This effect was overcome at later stages of infection (72 h and 96 h p.i.). In contrast to that, cells infected with the gpUS2–11pos strain RV-BADwt showed the well-known kinetics of pp65 peptide presentation (Besold et al., 2007), namely a marked impairment of presentation already at 24 h and a gradual decrease at later stages of infection. This was inversely correlated with the amount of pp65 protein, found in RV-BADwt infected cells, as visualized by quantitative Odyssey® infrared immunoblot. Infected cell lysates were probed with a pp65 specific monoclonal antibody and protein amount was normalized to β-actin (Fig. 6B).

To test, whether the effects of gpUS2 and gpUS11 were additive, HFF were also coinfected with RV-KB13 and RV-KB9. Surprisingly, there was an only slight reduction in spot numbers after coinfection, compared to that observed after infection with either one of the mutants (Fig. 6A). This indicates that gpUS2 and gpUS11 do not functionally cooperate in exporting HC from the ER, thereby suppressing MHC class I mediated peptide presentation at the cell surface. Taken together, these experiments showed that the expression of gpUS2 and gpUS11, alone or in combination, by HCMV infected cells was insufficient to prevent induction of IFN-γ secretion by pp65 specific CTL.

The experiments presented so far provided an apparent discrepancy. Expression of gpUS2 or gpUS11 in infected cells alone was sufficient to reduce HLA-A2 cell surface expression to basal levels, comparable to what was seen with the gpUS2–11pos wt virus RV-BADwt. In contrast, presentation of a peptide from pp65 by HLA-A2 was only slightly impaired at early times p.i. with US2pos or US11pos expressing viruses and showed no impairment at later stages of infection. Note that at late stages, HLA-A2 suppression, as measured by FACS was maximal for all viruses tested (Fig. 5A). One explanation for the dichotomy of HLA-A2 expression and $pp65_{NLV}$ presentation by

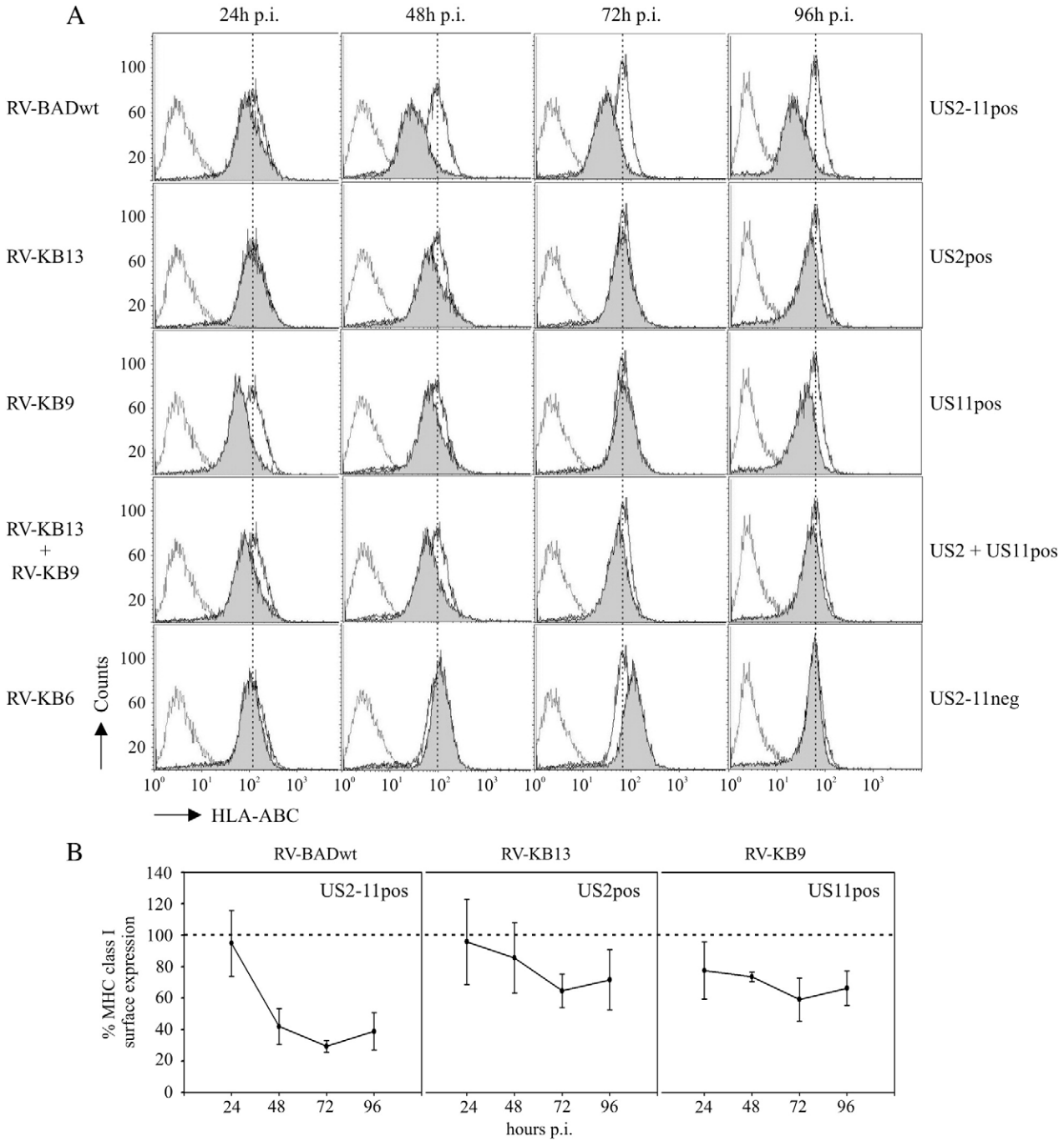

Fig. 4. Cytofluorometric analysis of MHC class I surface expression of HFF, infected with the recombinant viral strains. Cells were infected with viral inocula that were normalized for an uptake of 125 viral genomes per cell. At the indicated time points p.i., total MHC class I surface expression was measured using an HLA-ABC specific mAb for staining (clone W6/32). Antibody binding was visualized with FITC-conjugated polyclonal anti-mouse antibodies and analyzed by flow cytometry. Secondary antibody background staining was analyzed for each sample. Coinfection was performed using viral inocula of each one of the two viral strains that were normalized for an uptake of 125 viral genomes per cell. (A) Histogram blots of one representative experiment. Secondary antibody background staining is shown by dotted lines, staining of mock infected cells by solid lines and staining of infected cells by shaded graphs. Dashed vertical lines indicate the median of mock infected graphs at each time point p.i.. (B) Means and standard deviations of 3 independent experiments as shown in A. For each sample, the specific mean fluorescence intensity (MFI) was calculated by subtracting the background MFI (only secondary antibody) from the MFI obtained after staining with both primary and secondary antibodies. For each time point p.i. the specific MFI of RV-KB6 (US2–11neg) infected cells was defined as 100% MHC class I surface expression (shown as dashed line in the graph).

RV-KB13 and RV-KB9 infected cells was that FACS analysis of HLA-A2 was limited in its power to predict functional antigen presentation in general. Alternatively, it could be assumed that pp65 or the $pp65_{NLV}$ peptide was exceptional in a way to allow presentation despite the marked reduction of HLA-A2, seen by FACS. To test this, the MHC class I presentation of another antigen, the IE1 protein was investigated. Cells were infected with the different viruses and tested by Elispot for the presentation of the IE1 derived peptide TMYGGISLL ($IE1_{TMY}$; (Gallez-Hawkins et al., 2003), using a specific CTL clone [$IE1_{TMY}$-CTL; (Besold et al., 2007); Fig. 6A]. Again, the numbers of spots were calculated relative to the numbers obtained with cells, infected with the US2–11neg virus RV-KB6. As opposed to the presentation of $pp65_{NLV}$, the presentation of the IE1 derived peptide was significantly impaired in cells that were infected with the gpUS2pos or the

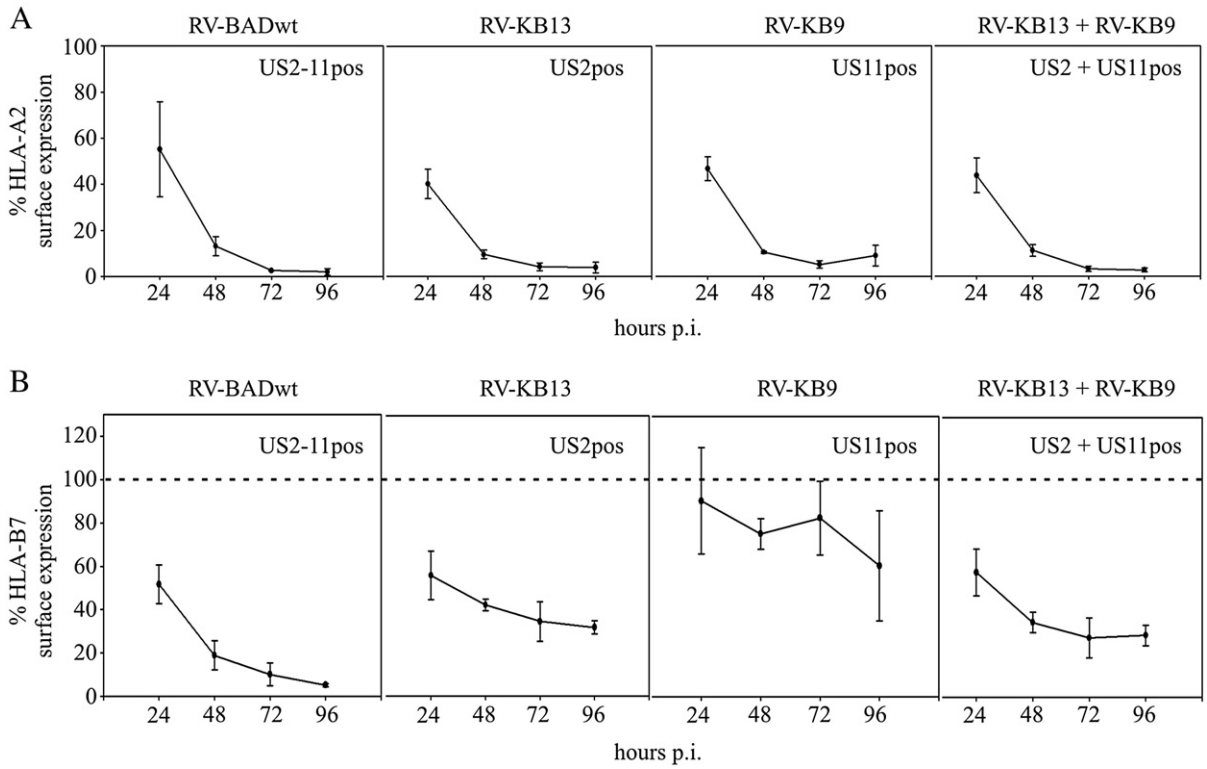

Fig. 5. Cytofluorometric analysis of HLA-A2 and -B7 surface expression of HFF, infected with the recombinant viral strains. HLA-A2- or HLA-B7-positive HFF were infected with an moi of 5 and, at the indicated time points p.i., incubated with HLA-A2 specific mAb (clone BB7.2) (A) or HLA-B7 specific mAb (clone BB7.1) (B) and PE-conjugated polyclonal anti-mouse antibodies. Subsequently, mean fluorescence intensities (MFI) were analyzed by flow cytometry. Secondary antibody background staining was quantified for each sample. For coinfection, each one of the viral strains was applied with an moi of 5. Means and standard deviations of 3 independent experiments are shown. For each sample, the specific MFI was calculated by subtracting the background MFI (only secondary antibody) from the MFI obtained after staining with both primary and secondary antibodies. For each time point p.i. the specific MFI of RV-KB6 (US2–11neg) infected cells was defined as 100% HLA-A2 (A) or -B7 (B) surface expression (shown as dashed line in graph B).

gpUS11pos mutants. No presentation at all was seen on RV-KB13 or RV-KB9 infected cells at 24 h p.i.. Some presentation became apparent, however, at later times. Coinfection with both viruses completely abrogated any measurable presentation of $IE1_{TMY}$. This was comparable to the well-known complete suppression of IE1 presentation on cells that were infected with a US2–11 competent wt virus like RV-BADwt that was used here (Besold et al., 2007; Gilbert et al., 1993; Manley et al., 2004). Similar results were obtained using a second HLA-A2 restricted CTL clone, directed against the IE1 derived peptide VLEETSVML [$IE1_{VLE}$; (Retiere et al., 2000); data not shown]. Suppression of IE1 presentation was in the face of significant levels of the IE1 protein in infected cells, as exemplified here using RV-BADwt infected HFF (Fig. 6B). These results indicated that both gpUS2 and gpUS11 were individually sufficient to suppress IE1 presentation at early times after infection. However, suppression appeared to become leaky at later stages, possibly correlating with the decrease in expression rates for US2 and US11 (see Fig. 3).

Fusion of $IE1_{TMY}$ to pp65 restores its presentation by gpUS11pos infected cells

CTL against $pp65_{NLV}$ are highly prevalent and can be found in high frequencies in individuals expressing the HLA-A2 allomorph. This peptide has consequently been labelled as being immunodominant (Elkington et al., 2003; Wills et al., 1996). Specific features of $pp65_{NLV}$, like efficiency of its generation by the proteasome or affinity to the HLA-A2 molecule may explain its presentation despite gpUS2 or gpUS11 expression in infected cells. Alternatively, special properties of the carrier molecule pp65 may have been the reason for the limited efficacy, by which gpUS2 and gpUS11 could suppress $pp65_{NLV}$ presentation. To analyze this, we used a previously established recombinant of HCMV (RV-VM3) which carries the $IE1_{TMY}$ peptide as integral part of pp65 (Mersseman et al., 2008a; Fig. 7A). This virus, based on the backbone of strain Ad169 derivative RV-HB5 (Borst et al., 1999) expresses only US11, but none of the three other evasin genes. We hypothesized that, if the characteristics of pp65 were important for the limited efficacy of gpUS11-mediated immune suppression, then the $pp65_{NLV}$ presentation phenotype should be transferable to $IE1_{TMY}$, expressed as part of the pp65 protein in RV-VM3 infected cells. Consequently, RV-VM3 infected cells (expressing the pp65-$IE1_{TMY}$ fusion protein) were analyzed by Elispot, using $IE1_{TMY}$-CTL and $pp65_{NLV}$-CTL as responder cells (Fig. 7B). Mutants RV-HB5 (Borst et al., 1999), RV-Hd65 (Besold et al., 2007) and RV-ΔUS2–11(Falk et al., 2002) were used for control (Fig. 7A). Cells infected with RV-HB5 showed no presentation of $IE1_{TMY}$ at 24 h p.i., as expected. Note that concordant with the results obtained with RV-KB9 some IE1-presentation became visible at later time points after infection (see Fig. 6A). In contrast, however, the $IE1_{TMY}$ was already presented at 24 h p.i. by RV-VM3 infected cells, and this presentation increased significantly throughout later phases of infection. These data showed that $IE1_{TMY}$ assumed the $pp65_{NLV}$ presentation phenotype in gpUS11 expressing infected cells. To investigate the levels of pp65-$IE1_{TMY}$ fusion protein and to exclude IE1-overexpression in RV-VM3 infected cells, a quantitative Odyssey® infrared immunoblot analysis was carried out. Infected cell lysates were probed with a pp65 specific monoclonal antibody. The amount of the fusion protein was normalized to β-actin (Fig. 7C). As expected, the amount of pp65-$IE1_{TMY}$ fusion protein increased substantially in the course of infection. This was consistent with the kinetics of pp65 expression during infection of HFF with an Ad169 derived strain, expressing the wt-pp65 (Fig. 6B, left). In contrast, the level of the IE1 protein remained at about the same level between 24–96 h p.i., excluding an enhanced IE1 expression in RV-VM3 infected cells as the cause for enhanced $IE1_{TMY}$ presentation. These findings showed that pp65 is an

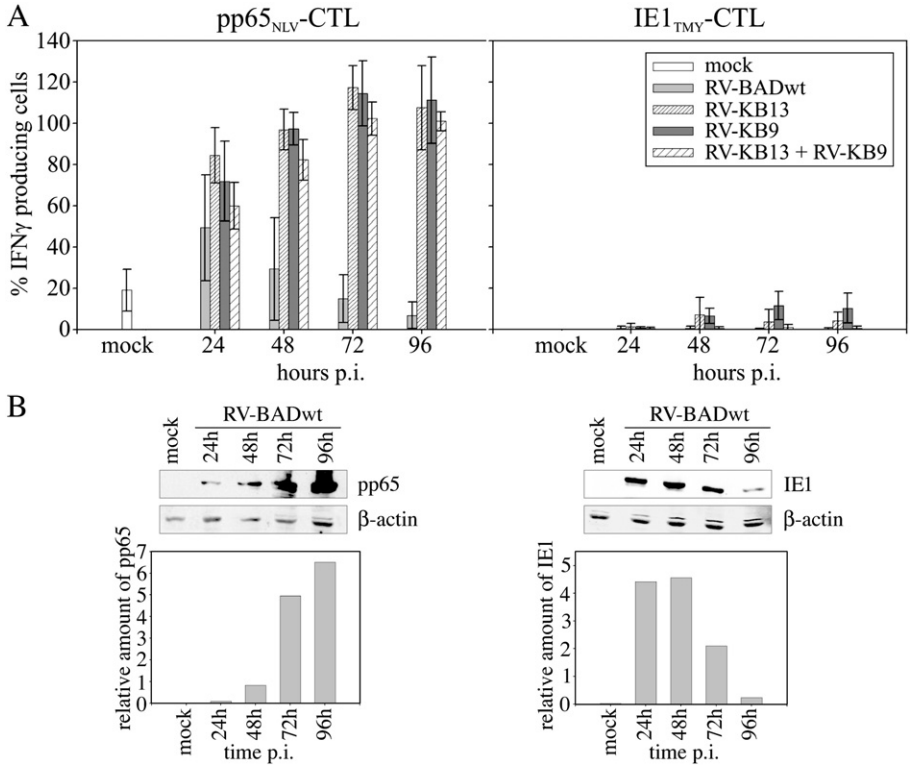

Fig. 6. (A) IFN-γ Elispot analysis of cells infected with the recombinant viral strains using $pp65_{NLV}$- (left panel) or $IE1_{TMY}$-CTL (right panel). HFF were either mock infected or infected at an moi of 5 with the recombinant viral strains and were analyzed for their HLA-A2 restricted $pp65_{NLV}$ and $IE1_{TMY}$ presentation. For coinfection, each of the viral strains was applied with an moi of 5. Means and standard deviations of 4 independent experiments are shown. For each time point p.i., the number of IFN-γ producing CTL that was obtained after infection with the US2–11neg virus RV-KB6 was taken as maximal value and was defined as 100%. (B) Quantitative Western blot analysis using the Licor Odyssey® infrared imaging system. HFF were either mock infected or infected at an moi of 5 with wild type strain RV-BADwt. At the indicated time points p.i., cell lysates were separated by SDS-PAGE and, after blotting, probed with mAb specific for pp65 (65-33) (left panel) and IE1 (p63-27) (right panel). A human actin specific polyclonal antiserum was used for normalization. To visualize primary antibody binding, infrared dye labelled secondary antibodies were used. Fluorescence intensities were measured using the Licor Odyssey® Software. To calculate relative amounts of both pp65 and IE1 content within infected cells for each time point p.i., the fluorescence intensity obtained after staining against each one of the two viral proteins was divided by the fluorescence intensity obtained after staining for actin.

exceptional CTL target antigen and that MHC class I presented peptides contained in this protein are only moderately suppressed by gpUS11.

Killing of RV-KB13 and RV-KB9 infected cells by human CTL

Expression of gpUS2 or gpUS11 by HCMV recombinants affected recognition by $pp65_{NLV}$-CTL and $IE1_{TMY}$-CTL to different levels. The biological relevance of the limited $IE1_{TMY}$ stimulation by late stage infected cells remained unclear in particular. We thus decided to perform a further experiment where we addressed the impact of gpUS2 and gpUS11 by recombinant viruses on cytotoxicity of pp65 and IE specific human T cell lines, using ^{51}Chromium release assays (CRA). We used CTL lines obtained from HCMV antibody seropositive, HLA-A2 positive donors to further provide evidence that the results obtained with murine CTL clones were relevant to human CTL recognition. These CTL lines were established as described previously (Weekes et al., 1999; Wills et al., 1996), using autologous PBMC, pulsed with either $pp65_{NLV}$ or the $IE1_{VLE}$. T cell lines were tested for peptide specific and HLA-A2 restricted cytotoxicity, using peptide pulsed autologous and mismatched EBV transformed B cells (not shown). These cytotoxic and HLA-A2 restricted T cell lines were used as effector cells in CRA against autologous, donor derived dermal HF, infected with RV-KB13 or RV-KB9 as target cells. Targets were infected at an moi of 10 for either 24 h or 72 h and were then subjected to a 20 hour CRA (Fig. 8). Cells infected with the gpUS2pos RV-KB13 or the gpUS11pos RV-KB9 were lysed at 72 h p.i., using pp65-specific human CTL lines. Yet the percentage of specific lysis was less, compared to that of cells infected with the gpUS2–11neg RV-KB6. In accordance, secretion of MIP1beta by the pp65-specific CTL into the culture supernatant, as measured by ELISA, was also reduced when RV-KB13 and RV-KB9 infected HF were used for stimulation (data not shown). These results indicate that, with respect to the CTL and the assay used for analysis, the relative impact of gpUS2 and gpUS11 on pp65-derived peptide presentation by MHC class I may vary.

As expected, cells infected with the US2–11neg RV-KB6 were efficiently killed by the $IE1_{VLE}$-CTL (Fig. 8). These CTL also killed HF infected with either RV-KB13 or RV-KB9, though, as was the case for pp65, to reduced levels, compared with RV-KB6. Killing was more pronounced, when HF were infected for 72 h. This was consistent with the results of the Elispot analyses, where only late stage infected cells were able to stimulate $IE1_{TMY}$-CTL (see Figs. 6 and 7). Surprisingly, even HF infected for 72 h with the US2–11pos parental strain RV-BADwt were killed to some extent by $IE1_{VLE}$-CTL, indicating that expression of all four immune evasins was insufficient to completely block recognition by IE1-specific CTL at late stages of infection. Taken together these experiments showed that gpUS2 and gpUS11 affect presentation of abundant viral proteins by MHC class I on HCMV infected cells, but that the sole expression of these viral evasins is insufficient to completely block CTL recognition in the course of infection of permissive HF.

Discussion

The functional relevance of the US2–11 gene locus for CTL recognition during HCMV infection is well documented by studies showing that CD8 T cells from infected individuals can be preferentially stimulated *ex vivo* by cells that are infected with a US2–11neg

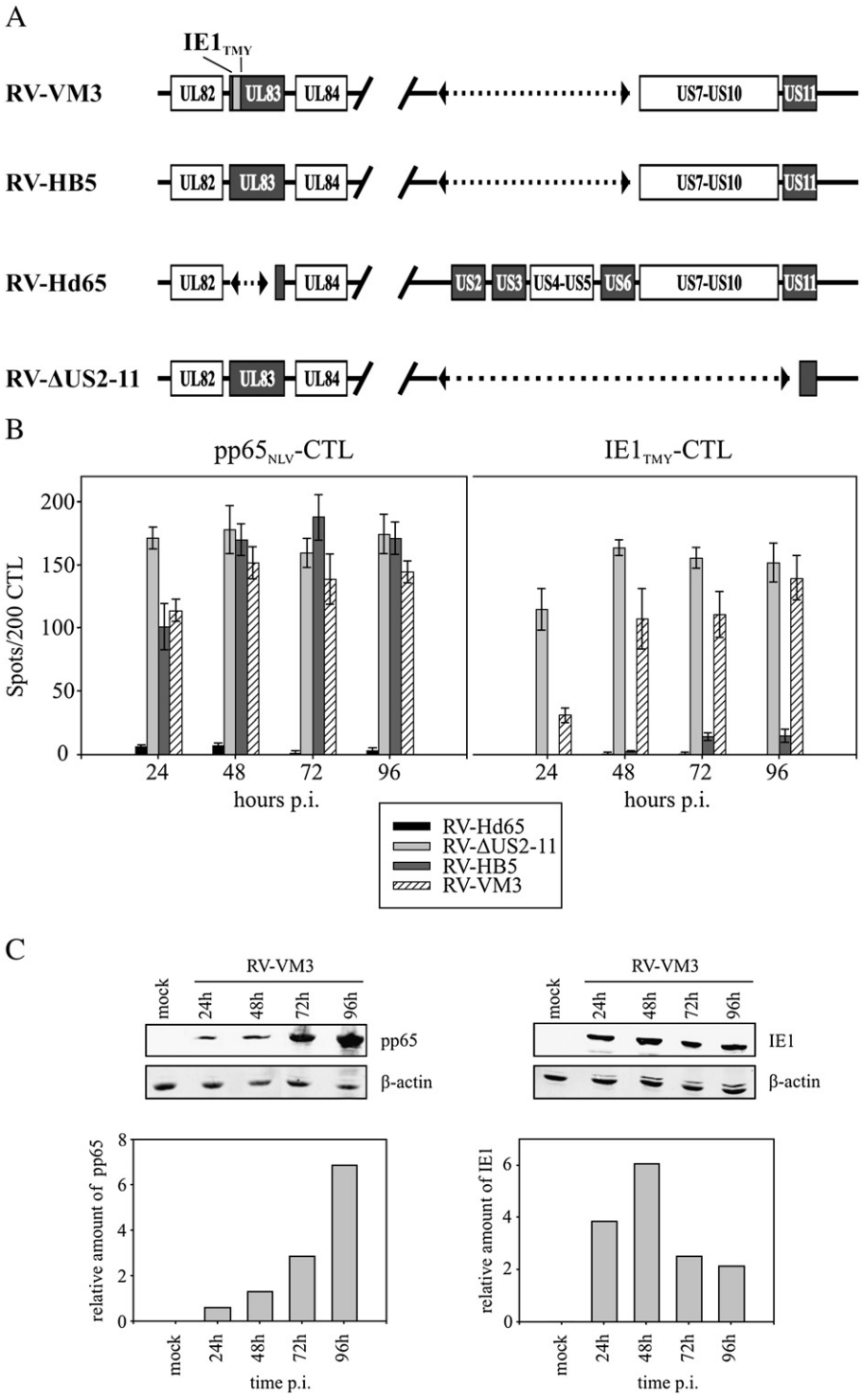

Fig. 7. Impact of gpUS11 on the presentation of IE_{TMY}, expressed as part of a pp65 fusion protein. (A) Schematic representation of viral strains, used for analysis. The location of the orfs encoding UL83 (pp65), US2, US3, US6 and US11 are shown by dark grey boxes. Dashed lines between arrowheads indicate deleted genomic regions. The position of the $IE1_{TMY}$ peptide within the primary structure of the pp65 fusion protein is indicated by a light grey box. (B) IFN-γ Elispot analysis of cells infected with the recombinant viral strains using $pp65_{NLV}$- (left panel) or $IE1_{TMY}$-CTL (right panel). HFF were infected at an moi of 5 with RV-HB5 or RV-VM3 and, at the indicated time points p.i., were analyzed for their HLA-A2 restricted $pp65_{NLV}$ and $IE1_{TMY}$ presentation. Infections with the pp65 deletion mutant RV-Hd65 and the immune evasion deletion mutant RV-ΔUS2–11 were used for negative and positive controls. Means and standard deviations of triplicate samples from one out of three independent experiments are shown. (C) Quantitative Western blot analysis using the Odyssey® infrared immunoblot imaging system. HFF were either mock infected or infected at an moi of 5 with the RV-VM3 mutant strain. At the indicated time points p.i., cell lysates were separated by SDS-PAGE and after blotting probed as described in Fig. 6B. Relative amounts of the viral proteins pp65 (left panel) and IE1 (right panel) within infected cells at each time point p.i. were calculated as described in Fig. 6B. RV-HB5, HCMV mutant, with a deletion in the US2–6 genes, which expresses gpUS11, but not gpUS2, 3 and 6. RV-VM3, HCMV mutant, based on RV-HB5 with an additional insertion of the $IE1_{TMY}$ peptide coding sequence in the UL83 gene, encoding pp65. RV-Hd65, HCMV mutant, with the coding sequence for the UL83 gene deleted. RV-ΔUS2–11, HCMV mutant with the genomic region encoding all genes between US2 and US11 deleted.

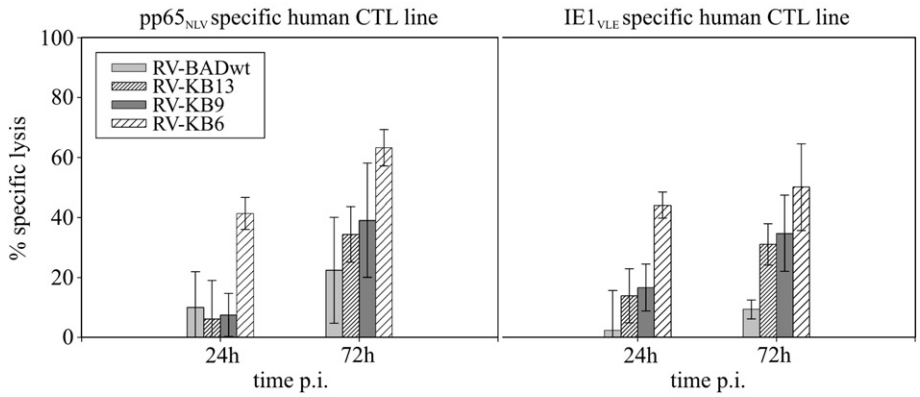

Fig. 8. Cytotoxicity assay using polyclonal $pp65_{NLV}$ (left panel) or $IE1_{VLE}$ (right panel) specific human CTL lines at an effector/target ratio of 100:1. Autologous human dermal fibroblasts (HF) were infected at an moi of 10 with the recombinant viral strains and at the indicated time points p.i. were used as targets in 20 h ^{51}Chromium release assay (CRA). Means and standard deviations of at least triplicate samples are shown.

virus (Khan et al., 2005; Manley et al., 2004). We could recently demonstrate that cells infected with a US2–11neg virus efficiently presented both IE1 and pp65 derived peptides (Besold et al., 2007). However, presentation of the same antigens was either completely abrogated (for IE1) or severely impaired (for pp65), when US2–11 genes were present in cells infected with the parental strain. Current opinion in the field is that the genes for US2–11 are sequentially expressed in the course of HCMV infection and that the proteins interfere with MHC class I biogenesis in a sequential manner (Ahn et al., 1996). However, it remained unclear, whether US2–11 cooperate in suppressing MHC I biogenesis or whether they can act widely independent in different phases of the HCMV replication cycle. One recent study using gpUS2/3 coexpression demonstrated that both proteins cooperate in suppressing MHC class I downregulation (Noriega and Tortorella, 2009). To address, how these findings relate to the role of US2–11 in their natural context of HCMV infection, it is essential to investigate the single members of these proteins individually and in various combinations in infected cells. Here we present, to our knowledge, the first study that focuses on the impact of individual evasins, namely gpUS2 and gpUS11 on functional MHC class I presentation of HCMV antigens in the course of infection.

During their pioneering studies, Jones and coworkers generated HCMV mutants that had a US2pos or a US11pos phenotype, but lacked the three other immune evasins (Jones et al., 1995; Jones and Sun, 1997). These mutants, however, were also deleted in the US4–5 and US7–10 open reading frames. Binding to MHC class I HC in the ER has been documented for the two ER-resident proteins encoded by US8 or US10 (Furman et al., 2002; Tirabassi and Ploegh, 2002) and at least the US10 gene product was found to delay MHC class I trafficking. Although expression of either US8 or US10 did not appear to modulate MHC class I surface expression (Ahn et al., 1997; Jones et al., 1995), an impact of these two proteins, or the other proteins encoded in this region during infection could not be excluded. We thus chose to establish a set of new mutants which had US4–5 and US7–10 retained.

The resulting viral mutants had to be thoroughly characterized, both genotypically and phenotypically. In particular, we could confirm that the release of progeny virus was unimpaired when three (RV-KB9, RV-KB13) or four (RV-KB6) of the evasins were absent. We further showed that the kinetics of viral DNA replication in cells infected with these mutants was widely unaltered. The latter issue had not been approached before and appears to be interesting considering the studies that reported influences of US3 on gene expression (Colberg-Poley et al., 1992). Our results indicate that the deletion of US3 has no severe impact on the ability of the virus to replicate its genome.

Infection with gpUS2pos and gpUS11pos viruses led to downregulation of HLA-ABC on infected HFF, as detected by flow cytometry. This showed that both proteins independently impair MHC class I surface expression on infected HF cells. The level of reduction was similar between the two viruses, but was less significant compared to cells infected with a strain that expressed all four immune evasins. This is in agreement with the model that gpUS2–11 work cooperatively to downregulate MHC class I. According to this, one of the four evasion proteins would not suffice to effect the same level of MHC class I attenuation as compared to their concerted action. Recent data from transient systems appear to support this model of cooperation (Noriega and Tortorella, 2009). HLA-A2 was more pronouncedly downregulated by cells infected with the gpUS2 and gpUS11 expressing viruses, compared to total HLA-ABC, showing kinetics and levels comparable to the gpUS2–11 competent virus. It thus appeared that gpUS2 and gpUS11 were each sufficient to mediate full downregulation of HLA-A2. As a matter of fact, both proteins have been shown to be effective in attacking HLA-A2, whereas they have been reported to be less effective against other HLA types (Barel et al., 2006). Consequently, the differences seen between HLA-ABC downregulation (Fig. 4) and HLA-A2 downregulation (Fig. 5) can be attributed to the different susceptibilities of the different HLA molecules to US2 and US11 mediated attack.

Downregulation of HLA-B7 surface expression on cells infected with US2pos and US11pos viruses was less intense, compared to that of HLA-A2. HLA-B7 expression was moderately reduced in cells infected with the US11pos virus. This is in accordance with results from others, showing that retroviral transduction of US11 leads to a roughly 50% reduction of HLA-B7 on transduced cells (Barel et al., 2006). We found, however, an even more pronounced downregulation of HLA-B7 on cells infected with the US2pos virus. This effect was not dependent on the fibroblast line used, as it could be confirmed using two additional HLA-B7 expressing lines (data not shown). The latter results appear to contrast with reports showing that gpUS2, expressed in transfected or retrovirally transduced cells failed to interact with HLA-B7 in the ER and was insufficient to downregulate HLA-B7 on the cell surface (Barel et al., 2003b, 2006; Gewurz et al., 2001b; Llano et al., 2003). The reasons for this discrepancy are not known at the current stage. The virus used in our analysis lacked all three other evasin genes, excluding influence by any one of the other immunomodulatory proteins gpUS3, gpUS6 or gpUS11. It has been shown that gpUS2 binds to HLA-A2 in a region between the peptide binding site and the α3-domain (Gewurz et al., 2001a). This region is not conserved in HLA-B7 and thus interaction was not observed using native gel shift analysis (Gewurz et al., 2001b). However, weak interactions may not be accessible by this kind of assay. Discrepant results with regard to the susceptibility of certain MHC class I alleles to gpUS2 attack have been ascribed to the different amounts of MHC molecules expressed in different cell types (Lilley and Ploegh, 2005). It is thus reasonable to assume that gpUS2 behaves differently when analyzed in the context of infection as opposed to its isolated

expression in uninfected cells of a different type. This underlines the importance to study the role of the immune evasion proteins in the context of infection in order to gain insight in their role in viral pathogenesis.

Cells infected with gpUS2 or gpUS11 expressing viruses were efficiently recognized by CTL specific for the HLA-A2 presented peptide $pp65_{NLV}$. This was an unexpected result, considering the efficient HLA-A2 downregulation at the same time p.i.. This indicates that despite low level HLA-A2 expression, as measured by flow cytometry, CTL may still bind to infected cells and may be activated to secrete cytokines and to kill their cognate target cells. Immunodominance of a given peptide could serve as an explanation for this. CTL against $pp65_{NLV}$ are found in high frequencies in HCMV seropositive individuals and this peptide is thus considered to be an immunodominant HLA-A2 presented antigen of the virus (Gillespie et al., 2000; Waller et al., 2007; Wills et al., 1996). In accordance with this, the $IE1_{TMY}$ was only barely presented in RV-KB13 or RV-KB9 infected cells, indicating that gpUS2 and gpUS11 were sufficient to suppress presentation of that particular subdominant peptide by HLA-A2. Interestingly, however, $IE1_{TMY}$ assumed the immunodominant phenotype of $pp65_{NLV}$ when expressed in fusion with pp65 (see Fig. 7). Consequently, the properties of the peptide alone may not be sufficient to explain the discrepancy between HLA-A2 surface expression and detectability by CTL. The viral protein that carries particular peptide epitopes may thus play a central role. Additional experiments are warranted to address this issue. One important message from this, however, is that measuring MHC class I surface expression on infected cells by flow cytometry does not necessarily correlate with functionally relevant antigen presentation. Consequently, for analyzing the role of immune evasion during HCMV infection, it is mandatory to include functional approaches like cytokine secretion or cytolysis assays.

Given the expression kinetics of US2 and US11, one would assume that these two genes significantly contribute to suppression of pp65 presentation by MHC class I. Indeed there was impairment both in cytokine secretion and cytolysis at 24 h p.i. when the gpUS2pos RV-KB13 or the gpUS11pos RV-KB9 was used for infection of HF. This suppressive effect was still visible in cytolysis assays using human CTL at 72 h p.i., but was abrogated in the Elispot analysis at that time point. It is likely that different experimental conditions account for this difference in suppression. In any way, the experimental setup employed to test for cytolysis using human CTL may well reflect certain conditions during natural infection of humans, when HCMV is replicating to high levels in infected organ tissues and cytotoxic T lymphocytes are attracted in larger numbers to the site of infection. Consequently it seems that both gpUS2 and gpUS11 alone have some effect on pp65 derived antigen presentation.

Cells infected with RV-KB13 or RV-KB9 did not stimulate IFNγ secretion by $IE1_{TMY}$-CTL at 24 h p.i. and induced only very limited numbers of spots at later time points. This indicated that gpUS2 and gpUS11 have a pronounced impact on the presentation of IE1 derived peptides. Surprisingly, however, CTL lines against the $IE1_{VLE}$ peptide, generated from human donors showed about 30% cytolysis of cells infected with RV-KB13 or RV-KB9 at 72 h p.i.. As discussed above the experimental setups used in both Elispot analysis and CRA cannot directly be compared; however, both approaches seem to indicate that, also for IE1, suppression of peptide presentation by gpUS2 and gpUS11 may be leaky at later times of HCMV infection. In line with this, the expression of both US2 and US11 RNA was barely detectable in Northern blots late in infection (Fig. 3). It thus is conceivable that a decrease of gpUS2 or gpUS11 (Ahn et al., 1996; Lilley and Ploegh, 2005) accounts for the recovery of pp65 and IE1 presentation in RV-KB13 and RV-KB9 infected cells.

The data presented here only refer to infected HF. It is unclear, what the impact of gpUS2 or gpUS11 would be on antigen presentation by other cell types, like professional antigen presenting cells. However, the primary goal of this analysis was to investigate, how MHC class I antigen presentation was impaired by US2 or US11 on highly permissive cell types, such as HF. It could be assumed, though not formally proven that the results obtained here may serve as a model for infected organ cells. Such cells are obviously major targets of CD8 T cells during the effector phase of the immune response. Consequently, the role of gpUS2 and gpUS11 for antigen presentation on these cells is of major interest, not only for our understanding of the functionality of these proteins; it may also aid to approaches to develop immunotherapeutic regimens against HCMV infection and disease.

In conclusion, we have shown here that gpUS2 and gpUS11 affect MHC class I presentation of HCMV infected cells in an antigen-dependent manner. The results suggest that immune evasion of MHC class I antigen presentation during HCMV infection is a dynamic process, which is governed by a delicate balance between the efficacy of the viral immunomodulatory proteins on the one hand and the ability of the infected cell to generate sufficient numbers of MHC class I complexes for cell surface presentation on the other hand. The work presented here provides a further step in our understanding of the roles of single members of the US2–11 genes in protecting HCMV from CTL recognition.

Materials and methods

Cells

Primary human foreskin fibroblasts (HFF) were grown in minimal essential medium (MEM; PAA, Cölbe, Germany), supplemented with 5–10% fetal calf serum (FCS; Biochrom, Berlin, Germany), 2 mM L-glutamin, 50 mg/l gentamycin and 0.5 ng/ml basic fibroblast growth factor (bFGF; Invitrogen, Karlsruhe, Germany). Autologous primary human fibroblasts were established and maintained as recently described (Waller et al., 2007).

CTL clones specific for the HLA-A0201 (A2) restricted HCMV derived peptides $pp65_{495–503}$ ($pp65_{NLV}$-CTL; Diamond et al., 1997; Wills et al., 1996) and $IE1_{297–305}$ ($IE1_{TMY}$-CTL; Gallez-Hawkins et al., 2003) were generated by peptide immunization of HLA-A2/huCD8 double-transgenic mice (a kind gift from L. Sherman, The Scipps Institute, La Jolla, CA, USA). Details of establishment and culturing of these cells were recently described (Besold et al., 2007).

Human CD8+ T cells were prepared from PBMC of HCMV antibody seropositive, HLA-A2 positive donors. In order to remove CD4+ T cells, CD19+ B cells, CD14+ monocytes and CD16+ NK cells, PBMC were stained with anti-CD4-, anti-CD19-, anti-CD14- and anti-CD16-FITC (Becton Dickinson, Oxford, UK) followed by anti-FITC conjugated MACS microbeads (Miltenyi Biotech, Surrey, UK) and passed through a MACS LS column (Miltenyi Biotech, Surrey, UK).

Polyclonal, peptide specific CTL lines were generated by stimulating MACS purified CD8+ T cells with irradiated autologous peptide-pulsed PBMC in RPMI medium, supplemented with 10% FCS, 10% human AB serum and 5 IU/ml recombinant human IL-2 (provided by the MRC Centralized Facility for AIDS Reagents, NIBSC, UK) and cultured for at least 14 days. CTL lines were maintained by splitting and feeding under the same conditions as mentioned above every 5 days.

Viruses

The HCMV strain RV-BADwt was reconstituted using the bacterial artificial chromosome (BAC) pAD/Cre [provided by Thomas Shenk; (Yu et al., 2002)]. This BAC contains the complete genome of the HCMV laboratory strain Ad169. In pAD/Cre, the BAC vector is inserted between the viral genes US28 and US29. Next to the vector sequence, an expression cassette for the Cre recombinase is contained. These heterologous sequences are flanked by LoxP sites. Transfection of pAD/Cre derived clones into HFF leads to the site-specific excision of

the BAC vector and the Cre gene, thereby minimizing non-viral sequences from the reconstituted viruses (Yu et al., 2002).

The recombinant viral strain RV-VM3 was generated by mutagenesis of the parental strain RV-HB5 (Borst et al., 1999). This virus expresses the $IE1_{297-305}$ ($IE1_{TMY}$) T-cell epitope fused to the pp65 protein (Mersseman et al., 2008a). In this virus, the BAC vector is inserted into the US2–US6 region of HCMV strain Ad169, thereby deleting these genes. For control purposes, the recombinant viruses RV-Hd65 (Besold et al., 2007) and RV-ΔUS2–11 (Falk et al., 2002) were employed.

To generate virus stocks, HFF were infected and incubated in a humidified, 5% CO_2 atmosphere at 37 °C for 5 to 8 days until the cultures displayed a complete cytopathic effect (CPE). Supernatants were cleared by centrifugation for 10 min at 3000 rpm and stored in aliquots at −80 °C. Virus stock titration was either performed by counting IE1 positive cells 48 h p.i., stained with a monoclonal antibody (mAb) against IE1 [p63-27; (Andreoni et al., 1989)] or by quantifying intracellular viral genomes 6 h p.i. by HCMV specific TaqMan PCR. Multiplicity of infection (moi) was defined as the number of IE1 positivity inducing units per cell. To correlate the moi with the number of intracellular viral genomes, HFF were infected with different mois. Six hours p.i. intracellular viral genomes were quantified by TaqMan PCR. Infection at an moi of 0.1 resulted in a number of roughly 4 intracellular viral genomes, infection at an moi of 5 in a number of roughly 125 intracellular viral genomes. For growth kinetics via TaqMan PCR, HFF were infected with viral inocula that were normalized for an equivalent uptake of 4 viral genomes per cell. For Northern blot analysis and for cytofluorometric analysis of MHC class I surface expression, HFF were infected with viral inocula normalized for an equivalent uptake of 125 viral genomes per cell. Cytofluorometric analyses of HLA-A2 and HLA-B7 surface expression, gamma interferon (IFN-γ) Elispot assays and Western blot analyses were performed using HFF infected at an moi of 5. For ^{51}Chromium release assays human fibroblasts (HF) were infected at an moi of 10.

BAC mutagenesis

Viral mutants were generated by BAC mutagenesis of the HCMV BAC pAD/Cre (Yu et al., 2002) using Red recombination in *E. coli* strain EL250 as described by Lee et al. (2001). For generation of BAC pKB6, the orfs US2, US3, US6 and US11 were sequentially deleted. In a first step (step 1), orf US2 was deleted by inserting a kanamycin resistance (Kan^R) gene. The Kan^R gene, flanked by FRT sites, was amplified from a derivative of vector pCP15 (Cherepanov and Wackernagel, 1995). In addition to the priming sequence for the Kan^R FRT cassette amplification, the oligonucleotides contained, at their very 5′-ends, about 50 bp of homology to the nucleotide sequences directly adjacent to US2. The complete sequences of the primers were as follows: (primer KB1: 5′-ATGGGTACTCGTGGCTAGATTTATTGAAATAAACCGCGATCCCG-GGCGTCTCGAGAAACGCAGCTTC-3′, and primer KB2: 5′-CTCTGGGA-TATAAATTGGGAAAGAGCGTACAGTCCACACGCTGTTTCACCGG-TACCCGGGGATCTTG-3′). After homologous recombination of the PCR product into the viral DNA, individual colonies were selected by addition of kanamycin. The Kan^R gene was then removed from the BAC of individual clones by site-specific Flp recombination at flanking FRT sites. For this, Flp expression was induced in *E. coli* EL250 by arabinose as originally described by Lee et al. (2001). The same strategy was then used in the second step (step 2) to remove US11. For this, primers with about 50 bp homology to the nucleotide sequences directly adjacent to US11 were used (primer KB7: 5′-GGTGAGTCGTTTCCGAGC-GACTCGAGATGCACTCCGCTTCAGTCTATATAGGTACCCGGGGATCTTG-3′, and primer KB8: 5′-TTACAGCTTTTGAGTCTAGACAGGGTAACAGCCTTC-CCTTGTAAGACAGATCGAGAAACGCAGCTTC-3′). Again, the Kan^R gene was removed by Flp recombination. For deletion of orf US3, in the third step (step 3), the Kan^R gene was used again, this time, however lacking flanking FRT sites. This strategy was chosen to avoid insertion of another FRT site into the HCMV genome. Therefore, one copy of the Kan^R gene is contained in the final BAC pKB6. The primers used for amplification were as follows: (primer KB3: 5′-GTACCTTGCAGCCCA-GGTAGGTTTCAGGTACCAGCTGGTTCGTACCTGGGAATAGGAACTTCAAG-ATCCCCC-3′, and primer KB4: 5′-GCAGCCAGACCGGAGCGGTGAGCGG-AGCCGAGCAGCGGACCTTCGGAGCCCAGAGCGCTTTTGAAGCTGGG-3′). Finally, for deletion of orf US6, in the fourth step (step 4), insertion of an ampicillin resistance gene (Amp^R) was used, which was also amplified from the derivative vector of pCP15 (primer KB5: 5′- GAGA-ATGCCGTGTTGAAGGAACGCGCTTTTATTGAGACGATAAAACAGCAGCG-GAACCCCTATTTGTT-3′, and primer KB6: 5′- GAACATATATAATCGCCGT-TTCGTAAGCACGTCGATATCACTCCTTCACTCTTGGTCTGACAGTTACC-3′).

To generate pKB13, the orfs US11, US3 and US6 were successively deleted, using steps 2, 3 and 4, as described above. To obtain pKB9, the orfs US2, US3 and US6 were successively deleted, using steps 1, 3 and 4 as described above. Reconstitution of BAC vector free wild type RV-BADwt and recombinant viruses RV-KB13, RV-KB9 and RV-KB6 was carried out as described by Yu et al. (2002). Successful BAC vector excision was controlled by PCR. For this, template viral DNA was isolated from supernatants of infected cells using the high pure viral nucleic acid kit according to the instructions of the manufacturer (Roche Diagnostics, Mannheim, Germany).

DNA, RNA and protein analyses

For restriction enzyme analysis of the recombinant BACs, DNA was isolated from 200 ml of overnight bacterial cultures using the Nucleobond AX 500 kit (Macherey-Nagel, Düren, Germany) according to the manufacturer's instructions. The DNA was digested with *Bam*HI for 6 h and separated on a 0.6% agarose gel at 60 V for 48 h. For Southern blot analyses, the DNA was transferred onto nylon membranes (Roche Diagnostics GmbH, Mannheim, Germany) and probed with DIG-11-dUTP labelled DNA probes specific for US2, US3, US6 and US11, respectively that were generated using the PCR DIG probe synthesis kit according to the instructions of the manufacturer (Roche Diagnostics). For generation of the probes, HCMV BAC pAD/Cre was used as template. Primers that hybridized to the orf US2 (KB28: 5′-ACCGCATCCACATCATAGAC-3′, and KB29: 5′-CCCGATGGAATCACT-AAAGC-3′), the orf US3 (KB30: 5′-TAAATCGCAGACGGGCGCTCAC-3′, and KB31: 5′-GCCGTCTTGTTCCTGAGACTCG-3′), the orf US6 (KB32: 5′-CAGGAGCCACAACGTCGAATC-3′, and KB33: 5′-CTCTGTCTCCGCGA-CAACAAG-3′) and the orf US11 (KB34: 5′-TGTCGGTGCAGCCAACCT-TTC-3′, and KB35: 5′-ACCGCCTCTGTCCGATGTTTC-3′) were used for amplification. Probes were between 550 and 650 bp, and thus covered large parts of the respective orfs.

For RNA preparation, cells were infected with viral inocula that were normalized for an uptake of 125 viral genomes per cell. The RNA was isolated using the RNeasy mini kit according to the manufacturer's instructions (Qiagen, Hilden, Germany). For Northern blot analyses, 8 μg total cellular RNA per lane was electrophoretically separated at 120 V for 5 h, using a 1% agarose gel, supplemented with 0.6% formaldehyde. RNA was transferred to nylon membranes (Roche Diagnostics) and probed with the same DIG-11-dUTP labelled DNA probes, specific for US2 and US11 that were also used for Southern blot. Southern and Northern blot analyses were performed according to the Roche DIG application manual for filter hybridization.

For quantitative Western blot analyses, infected or mock-infected cell lysates, obtained from 10^5 cells for each lane, were electrophoretically separated using 10% polyacrylamide gels containing 10% sodium dodecyl sulfate (SDS) and transferred to PVDF membranes (Immobilon-FL transfer membranes, Millipore, Schwalbach, Germany). SDS polyacrylamide gel electrophoresis and Western blotting were carried out as previously described (Schmolke et al., 1995). After blotting, membranes were blocked for 1 h using 0.2% I-Block (Applied Biosystems, distributed by Applera Deutschland GmbH, Darmstadt, Germany) in phosphate buffered saline (PBS). Primary

antibodies were diluted in 0.2% I-Block, supplemented with 0.1% Tween. Filters were incubated at room temperature overnight. Antibodies directed against pp65 (mAb 65-33) and IE1 [mAb p63-27; (Plachter et al., 1993)], both kindly provided by W. Britt, University of Alabama, Birmingham, AL, USA) were diluted 1:500, rabbit polyclonal antibody directed against actin (directed to amino acids 180 to 375 of human actin; Santa Cruz Biotechnology, Heidelberg, Germany) was diluted 1:200. After 3 washing steps in PBS, supplemented with 0.2% Tween, primary antibody binding was detected using infrared labelled secondary antibodies [IRDye 800 conjugated goat anti-mouse IgG (H + L); Rockland, Gilbertsville, PA, USA; distributed by Biotrend, Köln, Germany; Alexa Fluor 680 conjugated goat anti-rabbit IgG (H + L); Invitrogen, Karlsruhe, Germany]. Membranes were incubated in the dark for 1 h with secondary antibodies, diluted 1:10,000 in PBS supplemented with 0.1% Tween and 0.01% SDS. Using dual fluorescence, the detection of pp65 or IE1 on the one hand and cellular actin on the other hand could be performed on the same filter. Antibody binding was visualized using the Odyssey® infrared scanner (Licor Biosciences). Fluorescence intensities were quantified using the Licor Odyssey® Software. To calculate relative amounts of both pp65 and IE1 contents within infected cells, the fluorescence intensity obtained after staining against each one of the two viral proteins was divided by the fluorescence intensity obtained after actin staining.

Growth kinetics

For single step growth analyses, HFF were infected at an moi of 5 with the different viral strains. Aliquots of cell culture supernatants were harvested daily until complete cell lysis. IE1 forming units within the supernatants were quantified by counting IE1 positive cells 48 h p.i., stained with a monoclonal antibody (mAb) against IE1 [p63-27; (Andreoni et al., 1989)].

To quantify viral genomes accumulating within infected cells or released into the supernatant during infection, a quantitative real-time PCR using the TaqMan technology was performed. HFF were infected with viral inocula that were normalized for an uptake of 4 viral genomes per cell. At each of the following 5 (intracellular genomes) or 7 days (genomes released into the supernatant), viral genomes were isolated from 10^5 infected cells or from a 200 µl aliquot of the supernatant using the high pure viral nucleic acid kit (Roche Diagnostics) according to the manufacturer's recommendations. TaqMan PCR was performed in 50 µl reaction mixtures, containing 5 µl of either the viral DNA sample or standard DNA solution. Additional components were 2 units HotStarTaq DNA polymerase (Qiagen), 15 pmol of each primer and 5 pmol probe directed against the HCMV gene UL54, which was labelled with 6-carboxy-fluorescein reporter dye and 6-carboxy-tetramethyl-rhodamine quencher dye. The DNA standard for quantification was prepared by serial dilutions of 10^6 to 10 copies of cosmid pCM1049 (Fleckenstein et al., 1982). For thermal cycling, two initial steps of 2 min at 50 °C and 15 min at 95 °C were followed by 45 amplification cycles consisting of 15 s at 94 °C and 1 min at 60 °C. Real-time PCR was performed using an ABI Prism 7700 sequence detector (PE Applied Biosystems, Weiterstadt, Germany). For each DNA sample, PCR analysis was carried out in triplicates.

Flow cytometry

A fluorescence-activated cell sorter (FACSort, Becton Dickinson, San Jose, CA, USA) was used to analyze surface expression of MHC class I, HLA-A2 and HLA-B7 on HCMV infected HFF cells. 5×10^5 HFF were infected either at an moi of 5 or with viral inocula that were normalized for an uptake of 125 viral genomes per cell. In coinfection experiments, an moi of 5 or an infectious dose of 125 viral genomes was applied for each virus to ensure that expression levels of gpUS2 and gpUS11 were comparable to the levels obtained after infection with each individual mutant alone. Samples from 24, 48, 72 and 96 h p.i. were collected and washed in FACS buffer (PBS supplemented with 0.4% BSA, 10 mM EDTA and 20 mM HEPES). One half of the cells was stained using the respective primary antibody while the rest was mock stained with FACS buffer to detect secondary antibody background staining. Staining was performed for 30 min on ice in a final volume of 10–15 µl. For primary antibody staining, the HLA-ABC specific mAb clone W6/32 (Dako, Hamburg, Germany), the HLA-A2 specific mAb clone BB7.2 (BD Biosciences, Heidelberg, Germany) and the HLA-B7 specific mAb clone BB7.1 (AbD Serotec, Düsseldorf, Germany) were used in dilutions of 1:15 (anti-HLA-ABC), 1:10 (anti-HLA-A2) and 1:50 (anti-HLA-B7). After a washing step in FACS buffer, secondary antibody incubation was performed using a 1:15 dilution of FITC-conjugated polyclonal rabbit anti-mouse immunoglobulines (Ig) (Dako) or a 1:2 dilution of PE-conjugated goat F(ab′) anti-mouse IgG (R&D Systems, Wiesbaden-Nordenstadt, Germany). After an additional washing step, cells were resuspended in FACS buffer and subsequently subjected to cytofluorometric analysis.

Gamma interferon (IFN-γ) Elispot assay

Elispot assays were performed according to published procedures (Frankenberg et al., 2002; Miyahira et al., 1995). As stimulator cells, either mock or HCMV infected HFF were used. Infections were carried out at an moi of 5. For coinfection experiments, an moi of 5 was used for each virus. $Pp65_{NLV}$- and $IE1_{TMY}$-CTL clones served as responder cells (Besold et al., 2007). For each sample, 5×10^4 to 1×10^5 antigen presenting cells were probed with 200 responder cells. Triplicate samples were analyzed. Counting of spots was carried out using an SZX-12 microscope (Olympus, Hamburg, Germany).

Cytotoxicity assay

Peptide specific CTL lines were assayed for cytotoxicity against radiolabelled target cells in 20 h ^{51}Chromium release assays as previously described (Wills et al., 1996). Autologous fibroblasts were infected at an moi of 10 and were used 24 and 72 h p.i. as target cells for peptide specific CTL lines. Cytotoxicity assays were performed at an effector/target ratio of 100:1. For control, autologous fibroblasts and EBV transformed B cell lines pulsed with 40 µg/ml peptide were also used as target cells.

Acknowledgments

The technical assistance of M. Starke, S. Aue, N. Büscher and G. Okecha is gratefully appreciated. We are indebted to Thomas Shenk, Eva Borst, Martin Messerle, Gabriele Hahn and Ulrich Koszinowski for the donation of HCMV BACs, to Neal Copeland and Chiang Lee for bacterial strains, and to William Britt for monoclonal antibodies. This work was supported by grants from the Deutsche Forschungsgemeinschaft, Clinical Research Group 183, individual project 8 (B.P.), SFB 490, individual project E7 (B.P. and K.B.), and by the Maifor Program of the University Medical Center at the University of Mainz (K.B.). This study was also supported by a United Kingdom Medical Research Council Program Grant (M.W.).

References

Ahn, K., Angulo, A., Ghazal, P., Peterson, P.A., Yang, Y., Früh, K., 1996. Human cytomegalovirus inhibits antigen presentation by a sequential multistep process. Proc. Natl. Acad. Sci. U. S. A. 93, 10990–10995.

Ahn, K., Gruhler, A., Galocha, B., Jones, T.R., Wiertz, E.J., Ploegh, H.L., Peterson, P.A., Yang, Y., Früh, K., 1997. The ER-luminal domain of the HCMV glycoprotein US6 inhibits peptide translocation by TAP. Immunity 6, 613–621.

Andreoni, M., Faircloth, M., Vugler, L., Britt, W.J., 1989. A rapid microneutralization assay for the measurement of neutralizing antibody reactive with human cytomegalovirus. J. Virol. Methods 23, 157–167.

Barel, M.T., Pizzato, N., van, L.D., Bouteiller, P.L., Wiertz, E.J., Lenfant, F., 2003a. Amino acid composition of alpha1/alpha2 domains and cytoplasmic tail of MHC class I

molecules determine their susceptibility to human cytomegalovirus US11-mediated down-regulation. Eur. J. Immunol. 33, 1707–1716.
Barel, M.T., Ressing, M., Pizzato, N., van, L.D., Le, B.P., Lenfant, F., Wiertz, E.J., 2003b. Human cytomegalovirus-encoded US2 differentially affects surface expression of MHC class I locus products and targets membrane-bound, but not soluble HLA-G1 for degradation. J. Immunol. 171, 6757–6765.
Barel, M.T., Pizzato, N., Le, B.P., Wiertz, E.J., Lenfant, F., 2006. Subtle sequence variation among MHC class I locus products greatly influences sensitivity to HCMV US2- and US11-mediated degradation. Int. Immunol. 18, 173–182.
Barnes, P.D., Grundy, J.E., 1992. Down-regulation of the class I HLA heterodimer and beta 2- microglobulin on the surface of cells infected with cytomegalovirus. J. Gen. Virol. 73, 2395–2403.
Ben-Arieh, S.V., Zimerman, B., Smorodinsky, N.I., Yaacubovicz, M., Schechter, C., Bacik, I., Gibbs, J., Bennink, J.R., Yewdell, J.W., Coligan, J.E., Firat, H., Lemonnier, F., Ehrlich, R., 2001. Human cytomegalovirus protein US2 interferes with the expression of human HFE, a nonclassical class I major histocompatibility complex molecule that regulates iron homeostasis. J. Virol. 75, 10557–10562.
Besold, K., Frankenberg, N., Pepperl-Klindworth, S., Kuball, J., Theobald, M., Hahn, G., Plachter, B., 2007. Processing and MHC class I presentation of human cytomegalovirus pp65-derived peptides persist despite gpUS2–11-mediated immune evasion. J. Gen. Virol. 88, 1429–1439.
Böhm, V., Simon, C.O., Podlech, J., Seckert, C.K., Gendig, D., Deegen, P., Gillert-Marien, D., Lemmermann, N.A., Holtappels, R., Reddehase, M.J., 2008. The immune evasion paradox: immunoevasins of murine cytomegalovirus enhance priming of CD8 T cells by preventing negative feedback regulation. J. Virol. 82, 11637–11650.
Borst, E.M., Hahn, G., Koszinowski, U.H., Messerle, M., 1999. Cloning of the human cytomegalovirus (HCMV) genome as an infectious bacterial artificial chromosome in *Escherichia coli*: a new approach for construction of HCMV mutants. J. Virol. 73, 8320–8329.
Bouvier, M., 2003. Accessory proteins and the assembly of human class I MHC molecules: a molecular and structural perspective. Mol. Immunol. 39, 697–706.
Braud, V.M., Tomasec, P., Wilkinson, G.W., 2002. Viral evasion of natural killer cells during human cytomegalovirus infection. Curr. Top. Microbiol. Immunol. 269, 117–129.
Brune, W., Wagner, M., Messerle, M., 2006. Manipulating cytomegalovirus genomes by BAC mutagensis: strategies and applications. In: Reddehase, M.J. (Ed.), Cytomegaloviruses: Molecular Biology and Immunology. Caister Academic Press Ltd, Wymondham, Norfolk, U.K., pp. 63–89.
Chau, N.H., Vanson, C.D., Kerry, J.A., 1999. Transcriptional regulation of the human cytomegalovirus US11 early gene. J. Virol. 73, 863–870.
Cherepanov, P.P., Wackernagel, W., 1995. Gene disruption in *Escherichia coli*: TcR and KmR cassettes with the option of Flp-catalyzed excision of the antibiotic-resistance determinant. Gene 158, 9–14.
Colberg-Poley, A.M., Santomenna, L.D., Harlow, P.P., Benfield, P.A., Tenney, D.J., 1992. Human cytomegalovirus US3 and UL36–38 immediate-early proteins regulate gene expression. J. Virol. 66, 95–105.
Diamond, D.J., York, J., Sun, J.Y., Wright, C.L., Forman, S.J., 1997. Development of a candidate HLA A*0201 restricted peptide-based vaccine against human cytomegalovirus infection. Blood 90, 1751–1767.
Dunn, W., Chou, C., Li, H., Hai, R., Patterson, D., Stolc, V., Zhu, H., Liu, F., 2003. Functional profiling of a human cytomegalovirus genome. Proc. Natl. Acad. Sci. U. S. A. 100, 14223–14228.
Elkington, R., Walker, S., Crough, T., Menzies, M., Tellam, J., Bharadwaj, M., Khanna, R., 2003. Ex vivo profiling of CD8+-T-cell responses to human cytomegalovirus reveals broad and multispecific reactivities in healthy virus carriers. J. Virol. 77, 5226–5240.
Falk, C.S., Mach, M., Schendel, D.J., Weiss, E.H., Hilgert, I., Hahn, G., 2002. NK cell activity during human cytomegalovirus infection is dominated by US2–11-mediated HLA class I down-regulation. J. Immunol. 169, 3257–3266.
Fleckenstein, B., Müller, I., Collins, J., 1982. Cloning of the complete human cytomegalovirus genome in cosmids. Gene 18, 39–46.
Frankenberg, N., Pepperl-Klindworth, S., Meyer, R.G., Plachter, B., 2002. Identification of a conserved HLA-A2-restricted decapeptide from the IE1 protein (pUL123) of human cytomegalovirus. Virology 295, 208–216.
Furman, M.H., Dey, N., Tortorella, D., Ploegh, H.L., 2002. The human cytomegalovirus US10 gene product delays trafficking of major histocompatibility complex class I molecules. J. Virol. 76, 11753–11756.
Gallez-Hawkins, G., Villacres, M.C., Li, X., Sanborn, M.C., Lomeli, N.A., Zaia, J.A., 2003. Use of transgenic HLA A*0201/Kb and HHD II mice to evaluate frequency of cytomegalovirus IE1-derived peptide usage in eliciting human CD8 cytokine response. J. Virol. 77, 4457–4462.
Gewurz, B.E., Gaudet, R., Tortorella, D., Wang, E.W., Ploegh, H.L., Wiley, D.C., 2001a. Antigen presentation subverted: structure of the human cytomegalovirus protein US2 bound to the class I molecule HLA-A2. Proc. Natl. Acad. Sci. U. S. A. 98, 6794–6799.
Gewurz, B.E., Wang, E.W., Tortorella, D., Schust, D.J., Ploegh, H.L., 2001b. Human cytomegalovirus US2 endoplasmic reticulum-lumenal domain dictates association with major histocompatibility complex class I in a locus-specific manner. J. Virol. 75, 5197–5204.
Gilbert, M.J., Riddell, S.R., Li, C.R., Greenberg, P.D., 1993. Selective interference with class I major histocompatibility complex presentation of the major immediate-early protein following infection with human cytomegalovirus. J. Virol. 67, 3461–3469.
Gillespie, G.M., Wills, M.R., Appay, V., O'Callaghan, C., Murphy, M., Smith, N., Sissons, P., Rowland-Jones, S., Bell, J.I., Moss, P.A., 2000. Functional heterogeneity and high frequencies of cytomegalovirus- specific CD8(+) T lymphocytes in healthy seropositive donors. J. Virol. 74, 8140–8150.
Heemels, M.T., Ploegh, H., 1995. Generation, translocation, and presentation of MHC class I-restricted peptides. Annu. Rev. Biochem. 64, 463–491.
Hegde, N.R., Tomazin, R.A., Wisner, T.W., Dunn, C., Boname, J.M., Lewinsohn, D.M., Johnson, D.C., 2002. Inhibition of HLA-DR assembly, transport, and loading by human cytomegalovirus glycoprotein US3: a novel mechanism for evading major histocompatibility complex class II antigen presentation. J. Virol. 76, 10929–10941.
Jones, T.R., Muzithras, V.P., 1991. Fine mapping of transcripts expressed from the US6 gene family of human cytomegalovirus strain AD169. J. Virol. 65, 2024–2036.
Jones, T.R., Sun, L., 1997. Human cytomegalovirus US2 destabilizes major histocompatibility complex class I heavy chains. J. Virol. 71, 2970–2979.
Jones, T.R., Hanson, L.K., Sun, L., Slater, J.S., Stenberg, R.M., Campbell, A.E., 1995. Multiple independent loci within the human cytomegalovirus unique short region down-regulate expression of major histocompatibility complex class I heavy chains. J. Virol. 69, 4830–4841.
Jones, T.R., Wiertz, E.J., Sun, L., Fish, K.N., Nelson, J.A., Ploegh, H.L., 1996. Human cytomegalovirus US3 impairs transport and maturation of major histocompatibility complex class I heavy chains. Proc. Natl. Acad. Sci. U. S. A. 93, 11327–11333.
Khan, N., Bruton, R., Taylor, G.S., Cobbold, M., Jones, T.R., Rickinson, A.B., Moss, P.A., 2005. Identification of cytomegalovirus-specific cytotoxic T lymphocytes in vitro is greatly enhanced by the use of recombinant virus lacking the US2 to US11 region or modified vaccinia virus Ankara expressing individual viral genes. J. Virol. 79, 2869–2879.
Kollert-Jöns, A., Bogner, E., Radsak, K., 1991. A 15-kilobase-pair region of the human cytomegalovirus genome which includes US1 through US13 is dispensable for growth in cell culture. J. Virol. 65, 5184–5189.
Lee, E.C., Yu, D., Martinez, d.V., Tessarollo, L., Swing, D.A., Court, D.L., Jenkins, N.A., Copeland, N.G., 2001. A highly efficient *Escherichia coli*-based chromosome engineering system adapted for recombinogenic targeting and subcloning of BAC DNA. Genomics 73, 56–65.
Lilley, B.N., Ploegh, H.L., 2004. A membrane protein required for dislocation of misfolded proteins from the ER. Nature 429, 834–840.
Lilley, B.N., Ploegh, H.L., 2005. Viral modulation of antigen presentation: manipulation of cellular targets in the ER and beyond. Immunol. Rev. 207, 126–144.
Llano, M., Guma, M., Ortega, M., Angulo, A., Lopez-Botet, M., 2003. Differential effects of US2, US6 and US11 human cytomegalovirus proteins on HLA class Ia and HLA-E expression: impact on target susceptibility to NK cell subsets. Eur. J. Immunol. 33, 2744–2754.
Loenen, W.A., Bruggeman, C.A., Wiertz, E.J., 2001. Immune evasion by human cytomegalovirus: lessons in immunology and cell biology. Semin. Immunol. 13, 41–49.
Loureiro, J., Lilley, B.N., Spooner, E., Noriega, V., Tortorella, D., Ploegh, H.L., 2006. Signal peptide peptidase is required for dislocation from the endoplasmic reticulum. Nature 441, 894–897.
Manley, T.J., Luy, L., Jones, T., Boeckh, M., Mutimer, H., Riddell, S.R., 2004. Immune evasion proteins of human cytomegalovirus do not prevent a diverse CD8+ cytotoxic T-cell response in natural infection. Blood 104, 1075–1082.
Mersseman, V., Besold, K., Reddehase, M.J., Wolfrum, U., Strand, D., Plachter, B., Reyda, S., 2008a. Exogenous introduction of an immunodominant peptide from the non-structural IE1 protein of human cytomegalovirus into the MHC class I presentation pathway by recombinant dense bodies. J. Gen. Virol. 89, 369–379.
Mersseman, V., Bohm, V., Holtappels, R., Deegen, P., Wolfrum, U., Plachter, B., Reyda, S., 2008b. Refinement of strategies for the development of a human cytomegalovirus dense body vaccine. Med. Microbiol. Immunol. 197, 97–107.
Miyahira, Y., Murata, K., Rodriguez, D., Rodriguez, J.R., Esteban, M., Rodrigues, M.M., Zavala, F., 1995. Quantification of antigen specific CD8+ T cells using an ELISPOT assay. J. Immunol. Methods 181, 45–54.
Mocarski, E.S., 2004. Immune escape and exploitation strategies of cytomegaloviruses: impact on and imitation of the major histocompatibility system. Cell. Microbiol. 6, 707–717.
Mocarski, E.S., Shenk, T., Pass, R.F., 2007. Cytomegaloviruses. In: Knipe, D.M., Howley, P.M. (Eds.), Fields Virology. Lippincott Williams & Wilkins, Philadelphia, pp. 2701–2772.
Noriega, V.M., Tortorella, D., 2009. Human cytomegalovirus-encoded immune modulators partner to downregulate major histocompatibility complex class I molecules. J. Virol. 83, 1359–1367.
Plachter, B., Britt, W.J., Vornhagen, R., Stamminger, T., Jahn, G., 1993. Analysis of proteins encoded by IE-regions 1 and 2 of human cytomegalovirus using monoclonal antibodies generated against recombinant antigens. Virology 193, 642–652.
Powers, C., DeFilippis, V., Malouli, D., Früh, K., 2008. Cytomegalovirus immune evasion. Curr. Top. Microbiol. Immunol. 325, 333–360.
Reddehase, M.J., 2002. Antigens and immunoevasins: opponents in cytomegalovirus immune surveillance. Nat. Rev., Immunol. 2, 831–844.
Reddehase, M.J., Mutter, W., Münch, K., Bühring, H.J., Koszinowski, U.H., 1987. CD8-positive T lymphocytes specific for murine cytomegalovirus immediate-early antigens mediate protective immunity. J. Virol. 61, 3102–3108.
Rehm, A., Engelsberg, A., Tortorella, D., Korner, J., Lehmann, I., Ploegh, H.L., Hopken, U.E., 2002. Human cytomegalovirus gene products US2 and US11 differ in their ability to attack major histocompatibility class I heavy chains in dendritic cells. J. Virol. 76, 5043–5050.
Retiere, C., Prod'homme, V., Imbert-Marcille, B.M., Bonneville, M., Vie, H., Hallet, M.M., 2000. Generation of cytomegalovirus-specific human T-lymphocyte clones by using autologous B-lymphoblastoid cells with stable expression of pp65 or IE1 proteins: a tool to study the fine specificity of the antiviral response. J. Virol. 74, 3948–3952.
Schmolke, S., Drescher, P., Jahn, G., Plachter, B., 1995. Nuclear targeting of the tegument protein pp65 (UL83) of human cytomegalovirus: an unusual bipartite nuclear localization signal functions with other portions of the protein to mediate its efficient nuclear transport. J. Virol. 69, 1071–1078.
Schust, D.J., Tortorella, D., Seebach, J., Phan, C., Ploegh, H.L., 1998. Trophoblast class I major histocompatibility complex (MHC) products are resistant to rapid degradation

imposed by the human cytomegalovirus (HCMV) gene products US2 and US11. J. Exp. Med. 188, 497–503.
Simon, C.O., Holtappels, R., Tervo, H.M., Böhm, V., Däubner, T., Oehrlein-Karpi, S.A., Kühnapfel, B., Renzaho, A., Strand, D., Podlech, J., Reddehase, M.J., Grzimek, N.K.A., 2006. CD8 T cells control cytomegalovirus latency by epitope-specific sensing of transcriptional reactivation. J. Virol. 80, 10436–10456.
Sinzger, C., Grefte, A., Plachter, B., Gouw, A.S.H., The, T.H., Jahn, G., 1995. Fibroblasts, epithelial cells, endothelial cells and smooth muscle cells are major targets of human cytomegalovirus infection in-vivo. J. Gen. Virol. 76, 741–750.
Tirabassi, R.S., Ploegh, H.L., 2002. The human cytomegalovirus US8 glycoprotein binds to major histocompatibility complex class I products. J. Virol. 76, 6832–6835.
Tomazin, R., Boname, J., Hegde, N.R., Lewinsohn, D.M., Altschuler, Y., Jones, T.R., Cresswell, P., Nelson, J.A., Riddell, S.R., Johnson, D.C., 1999. Cytomegalovirus US2 destroys two components of the MHC class II pathway, preventing recognition by CD4+ T cells. Nat. Med. 5, 1039–1043.
Tortorella, D., Gewurz, B.E., Furman, M.H., Schust, D.J., Ploegh, H.L., 2000. Viral subversion of the immune system. Annu. Rev. Immunol. 18, 861–926.
Townsend, A., Ohlen, C., Bastin, J., Ljunggren, H.G., Foster, L., Karre, K., 1989. Association of class I major histocompatibility heavy and light chains induced by viral peptides. Nature 340, 443–448.
Waller, E.C., McKinney, N., Hicks, R., Carmichael, A.J., Sissons, J.G., Wills, M.R., 2007. Differential costimulation through CD137 (4-1BB) restores proliferation of human virus-specific "effector memory" (CD28(−) CD45RA(HI)) CD8(+) T cells. Blood 110, 4360–4366.
Walter, E.A., Greenberg, P.D., Gilbert, M.J., Finch, R.J., Watanabe, K.S., Thomas, E.D., Riddell, S.R., 1995. Reconstitution of cellular immunity against cytomegalovirus in recipients of allogeneic bone marrow by transfer of T-cell clones from the donor. N. Engl. J. Med. 333, 1038–1044.
Weekes, M.P., Wills, M.R., Mynard, K., Carmichael, A.J., Sissons, J.G., 1999. The memory cytotoxic T-lymphocyte (CTL) response to human cytomegalovirus infection contains individual peptide-specific CTL clones that have undergone extensive expansion in vivo. J. Virol. 73, 2099–2108.
Wiertz, E.J., Jones, T.R., Sun, L., Bogyo, M., Geuze, H.J., Ploegh, H.L., 1996a. The human cytomegalovirus US11 gene product dislocates MHC class I heavy chains from the endoplasmic reticulum to the cytosol. Cell 84, 769–779.
Wiertz, E.J., Tortorella, D., Bogyo, M., Yu, J., Mothes, W., Jones, T.R., Rapoport, T.A., Ploegh, H.L., 1996b. Sec61-mediated transfer of a membrane protein from the endoplasmic reticulum to the proteasome for destruction. Nature 384, 432–438.
Wills, M.R., Carmichael, A.J., Mynard, K., Jin, X., Weekes, M.P., Plachter, B., Sissons, J.G., 1996. The human cytotoxic T-lymphocyte (CTL) response to cytomegalovirus is dominated by structural protein pp65: frequency, specificity, and T-cell receptor usage of pp65- specific CTL. J. Virol. 70, 7569–7579.
Yewdell, J.W., Bennink, J.R., 2001. Cut and trim: generating MHC class I peptide ligands. Curr. Opin. Immunol. 13, 13–18.
Yu, D., Smith, G.A., Enquist, L.W., Shenk, T., 2002. Construction of a self-excisable bacterial artificial chromosome containing the human cytomegalovirus genome and mutagenesis of the diploid TRL/IRL13 gene. J. Virol. 76, 2316–2328.